



# 1 Redefining dangerous glacial lakes in Bhutan by integrating hydrodynamic flood 2 mapping and downstream exposure data

3 Sonam Rinzin<sup>1</sup>, Stuart Dunning<sup>1</sup>, Rachel Joanne Carr<sup>1</sup>, Simon Allen<sup>2</sup>, Sonam Wangchuk<sup>3</sup>  
4 and Ashim Sattar<sup>4</sup>

5 <sup>1</sup>School of Geography, Politics and Sociology, Newcastle University, Newcastle upon Tyne,  
6 UK

7 <sup>2</sup>Department of Geography, University of Zurich, Zurich, Switzerland

<sup>8</sup> <sup>3</sup>International Centre for Integrated Mountain Development, Kathmandu, Nepal

9 <sup>4</sup>School of Earth, Ocean and Climate Sciences, Indian Institute of Technology Bhubaneswar,  
10 Bhubaneswar, Odisha, India

11

12 Correspondence: Sonam Rinzin (s.rinzin2@newcastle.ac.uk)

## 13 Abstract

Dangerous glacial lakes in Bhutan have primarily been identified considering the likelihood of producing a GLOF, which in turn has been assessed only based on upstream lake area/volume and their surrounding topographic conditions. However, this approach is incomplete as it ignores the at-risk downstream exposure and vulnerability thus the actual impacts. Here we redefined dangerous glacial lakes by considering the impact of the simulated most likely scenario GLOF on downstream exposed elements at risk. Our study shows that a total of approximately 22399 people, 2613 buildings, 270 km of road, 402 bridges and 20 km<sup>2</sup> of farmland are exposed to potential GLOF inundation in Bhutan. We classified lake130 (Thorthormi Tsho) as a very high danger glacial lake in Bhutan, five lakes as high danger and 21 other lakes as moderate danger. Among these high danger glacial lakes, three of them: lake93 (Phudung Tsho), lake251, and lake278 (Wonney Tsho) were not recognized as dangerous in previous studies. Our assessment further revealed five downstream local government administrative units (LGUs) are associated with very high GLOF danger while nine others are associated with high GLOF danger. Six of these LGUs had not been previously documented as being at risk from GLOF including: Chhoekhor and Bumthang town in Bumthang, Paro town and Lamgong in Paro, Nubi in Trongsa and Khoma in Lhuentse districts. Our study underscores the significance of integrating potential inundation mapping and downstream exposure data to define dangerous glacial lakes. We recommend strengthening and expanding the existing GLOF disaster preparedness and risk mitigation efforts in Bhutan to reduce future damage and loss in high GLOF danger LGUs identified in this study.



34 **1. Introduction**

35 There are currently 110,000 glacial lakes globally, with a total area of ~15,000 km<sup>2</sup>. These  
36 glacial lakes have increased in area by ~22% between 1990 and 2020, primarily due to  
37 addition of water from the melting of glaciers (Zhang et al., 2024). Glacial lakes across the  
38 world have produced 3152 GLOF events between 850 and 2022 C.E (Lützow et al., 2023),  
39 which caused more than 12,400 human deaths and damaged infrastructure worth hundreds  
40 of millions of USD (Carrivick and Tweed, 2016; Lützow et al., 2023). In HMA, 682 GLOF events  
41 occurred between 1833 and 2022, causing 6,907 fatalities (Shrestha et al., 2023) although  
42 over 80% of all casualties recorded in HMA are attributed to a single compounding event  
43 involving Chorabari Lake in 2013 (Allen et al., 2015; Das et al., 2015). Moraine-dammed GLOF  
44 events have caused an order of magnitude greater damage than the combined damage from  
45 all other types of glacial lakes, despite moraine-dammed GLOF events only accounting for  
46 one-third of total GLOF events in HMA (Shrestha et al., 2023). One main reason is because  
47 moraine-dammed lakes are usually located nearer to human settlement than other types of  
48 glacial lakes, such as ice-dammed or supraglacial ponds/lakes making it important to quantify  
49 the danger it poses to the downstream settlement (Carrivick and Tweed, 2016).

50 Existing dangerous glacial lakes (DGLs) in Bhutan are defined based on how likely and  
51 magnitude of GLOF they will produce, which in turn are assessed based on the inherent  
52 stability of the lake's dam and factors that influence the potential for an external triggering  
53 event, such as a mass movement entering lake (Allen et al., 2017; Zheng et al., 2021b).  
54 Commonly used parameters include topographic potential for mass input into the lake from  
55 the surrounding hillslopes, lake volume (usually derived from a relationship to lake area), lake  
56 growth, moraine dam geometry and composition, and catchment area (Zhang et al., 2023b;  
57 Zheng et al., 2021b). Although the approaches and factors selected are influenced by study  
58 objectives and expert judgment, they largely are based on historical events, often backed with  
59 limited observed data (Shrestha et al., 2023). Constraining certain parameters, such as the  
60 location and magnitude of possible/probable mass movements entering a lake, is challenging  
61 even with field-based assessments and more so when using coarse, globally available, open-  
62 access data, but the previous study shows that this may be fundamental in the resultant GLOF  
63 magnitude (Rinjin et al., 2025). Moreover, the dynamic nature of cryosphere processes,  
64 exacerbated under climate warming, means that these reconstructed GLOF characteristics  
65 cannot necessarily be applied to contemporary or future conditions (Allen et al., 2017). This is  
66 evident from some GLOF events which have occurred from glacial lakes which were deemed  
67 less susceptible to GLOF, for example, Lagmale glacial lake in Nepalese Himalaya in 2017  
68 (Byers et al., 2018) and Gongbatongsha Co lake in 2013 in Indian Himalaya (Cook et al.,  
69 2018). Thus, the likelihood of producing a GLOF from any glacial lake is subject to inevitable



70   uncertainties. Most importantly, DGLs defined solely based on GLOF susceptibility of the lake  
71   overlooks how the hydrodynamic properties of a possible GLOF interact with downstream  
72   exposure and vulnerability. If a glacial lake generates an exceptionally large flood, but the  
73   downstream community is unaffected, we can consider the danger from the glacial lake as  
74   low, whereas even a 'small' flood that impacts large number of people should be classified as  
75   high danger. Typically, this is neglected in favour of classifications of danger based only on  
76   lake/trigger conditions, and not downstream impacts (Taylor et al., 2023a).

77   In recent decades, the amount of infrastructure, buildings and farmland exposed to potential  
78   GLOFs in HMA has increased (Nie et al., 2023). For example, critical infrastructure, such as  
79   hydroelectric power plants are being developed closer to glacial lakes due to growing energy  
80   demand in HMA regions (Nie et al., 2021; Schwanghart et al., 2016). In HMA, the population  
81   in GLOF-exposed areas increased by 0.31% (7.0 million to 9.2 million) between 2000 and  
82   2020 and may therefore have contributed significantly more towards rising GLOF danger than  
83   (debatably) increasing GLOF magnitude due to lake expansion (Taylor et al., 2023b). Thus,  
84   changing downstream exposure and vulnerability can play a greater role in shaping  
85   contemporary and near-future GLOF risk than the glacial lake and surrounding properties,  
86   making the inclusion of the former in the identification of dangerous lakes a crucial, but often  
87   overlooked, factor both in the HMA and other high GLOF risk regions globally, such as the  
88   Andes (Cook et al., 2016; Colavitto et al., 2024).

89   To identify DGLs with greater confidence and to implement effective management, mitigation  
90   and/or emergency response, we need to consider the interaction between GLOF flow  
91   hydrodynamics, downstream exposure and vulnerability. Taylor et al. (2023a) used  
92   downstream population within a 1 km buffer of the river through which a GLOF would flow, to  
93   a maximum runout of 50 km from each glacial lake to calculate global scale GLOF danger.  
94   However, the coarse resolution of data and crude assumption of GLOF flow path without  
95   hydrodynamic modelling introduces substantial uncertainties due to factors such as detailed  
96   local topography, especially where even populations very close in plain view distance to a  
97   GLOF flow routeway are in reality disconnected from the river by, for example, high river  
98   terraces, which are common in high-mountain region such as Bhutan. GLOF risk  
99   assessments at the HMA scale have been done by combining hydrodynamic modelling and  
100   open-source downstream data, such as OpenStreetMap (Zhang et al., 2023b). Yet, they  
101   conducted flood mapping only for the glacial lakes that they deemed very high or high danger  
102   through prior GLOF susceptibility assessment. This means that flood mapping for some of the  
103   lakes that can directly impact the downstream communities in case of the future GLOF event  
104   from these lakes have been not carried out despite huge deviation and inconsistencies



105 between previous susceptibility assessments (Zheng et al., 2021b; Zhang et al., 2023b; Rinzin  
106 et al., 2021; National Centre for Hydrology and Meteorology [NCHM] , 2019). Previous  
107 example of GLOF events from the low GLOF susceptible lake impacting downstream  
108 community underscores uncertainty of these prior GLOF susceptibility assessment (Byers et  
109 al., 2018). Moreover, since such studies are focused on a global to continental scale, they do  
110 not provide adequate granularity at the national and basin scale for bespoke risk reduction  
111 activities and planning.

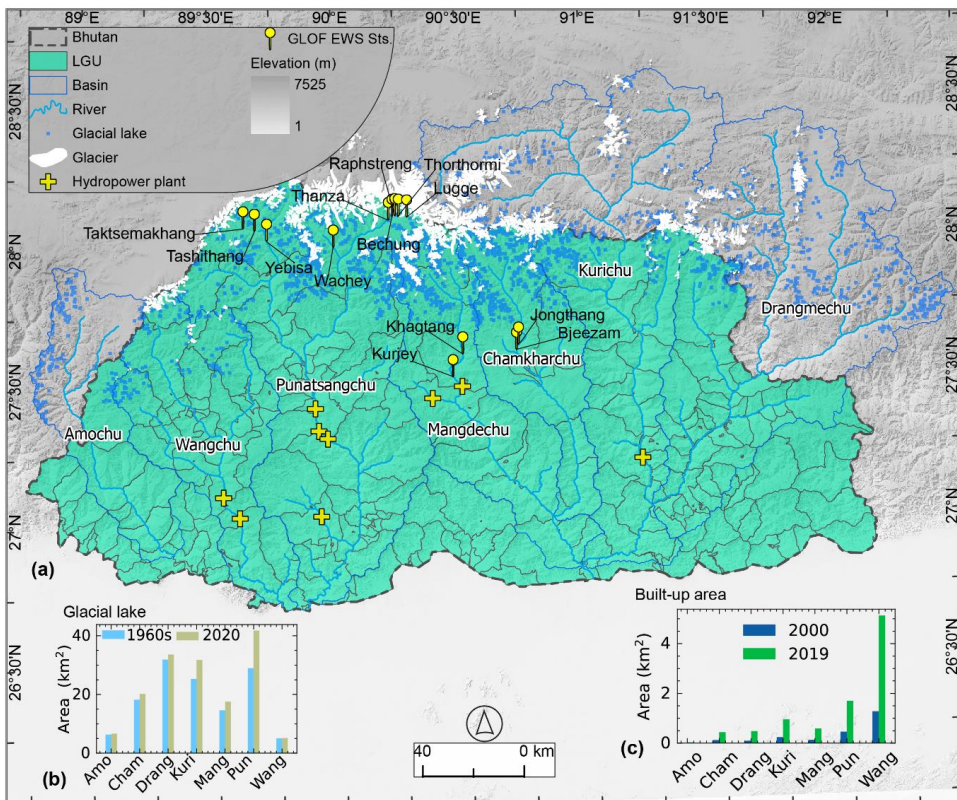
112 This study presents a new GLOF danger assessment approach for Bhutan, which combines  
113 robust flood mapping (through hydrodynamic modelling) and downstream exposure and  
114 vulnerability data. For this, we selected all glacial lakes with an area of 0.05 km<sup>2</sup> (n=278) within  
115 the Bhutan Himalaya and conducted hydrodynamic simulation for all these lakes using HEC-  
116 RAS (U.S. Army Corps of Engineers, 2021). We then combined the flood map generated  
117 through hydrodynamic modelling with downstream data on exposure and vulnerability derived  
118 from OpenStreetMap, land use and land cover maps and population and housing 2017 census  
119 data (National Statistics Bureau of Bhutan [NSB], 2018). As a result, 1) we produced a flood  
120 map for each glacial lake in Bhutan above 0.05 km<sup>2</sup>; 2) mapped all downstream exposed  
121 elements; and 3) provide a new, updated ranking of glacial lakes in Bhutan, based on the  
122 danger they pose to downstream settlement(s). We have developed a publicly available web  
123 portal that hosts the glacial lake dataset, GLOF flood maps and downstream GLOF risks  
124 across local administrative units in Bhutan.

## 125 **2. Study area**

126 Bhutan's landscape is characterised by high mountains, rugged topography and steep terrain  
127 with elevations ranging between 200 m a.s.l in the south to over 7000 m a.s.l in the north.  
128 Bhutan's northern regions consist of the greater Himalaya mountains, which contain ~1,487  
129 km<sup>2</sup> of glacier ice, of which 64% (951 km<sup>2</sup>) are debris-covered glaciers (Nagai et al., 2016)  
130 (Fig. 1). Between 2000 and 2020, Bhutanese glaciers lost mass at a rate of 0.47 m w.e. yr<sup>-1</sup>,  
131 which exceeds the neighbouring eastern Himalayan (~0.33 m w.e. yr<sup>-1</sup>) and Nyainqêntanglha  
132 (~0.46 m w.e. yr<sup>-1</sup>) regions (Hugonnet et al., 2021). It is projected that Bhutanese glaciers will  
133 undergo continuous and accelerated melting in the future in response to the current climate  
134 warming trend (Rupper et al., 2012). As of 2020, there were 2,574 (156.63 ± 7.95 km<sup>2</sup>) glacial  
135 lakes in Bhutan, which was an increase of 17.7% in number and 20.3% in area from the 1960s  
136 (Rinzin et al., 2021) (Fig. 1). While these glacial lakes are predominantly present in basins  
137 such as Phochu (28.18% of the total lake area), and Kurichu (26.35 % of the total area), they  
138 are widespread across the Bhutan Himalaya and drainage from these lakes flow across most  
139 of the major towns and settlements in Bhutan (Fig. 1). Of these glacial lakes, 64 were identified



140 as highly or very highly susceptible to producing GLOF in the future based on  
141 geomorphological conditions such as topographical potential for avalanching into the lake  
142 (Rinzin et al., 2021).



143  
144 **Figure 1.** The map (a) depicts Bhutan and the glaciated basin from which the river flows into  
145 inland Bhutan. It also shows the distribution of glacial lakes, glaciers, GLOF early warning  
146 monitoring stations (with name of the placed they are located at), and hydropower plants. The  
147 inset bar charts illustrate (b) glacial lake area of the 1960s and 2020 (Rinzin et al., 2021) and  
148 (c) built-up area changes between 200 and 2021 as per the land cover and landuse map of  
149 ICIIMOD (Uddin et al., 2021). The basin names are presented in their abbreviated form x-tick  
150 labels for both bar charts.

151 The glaciers in the northern mountains feed seven major river systems in Bhutan namely  
152 (West-East): Amochu, Wangchu, Punatsangchu, Mangdechu, Chamkharchu, Kurichu and  
153 Drangmechu (Fig. 1). The hydropower generated from these river systems accounts for about  
154 40% of Bhutan's national revenue to a value of 0.27 billion USD (Ministry of Economic Affairs,  
155 2021) as significant power is exported to India. All seven currently operational hydropower

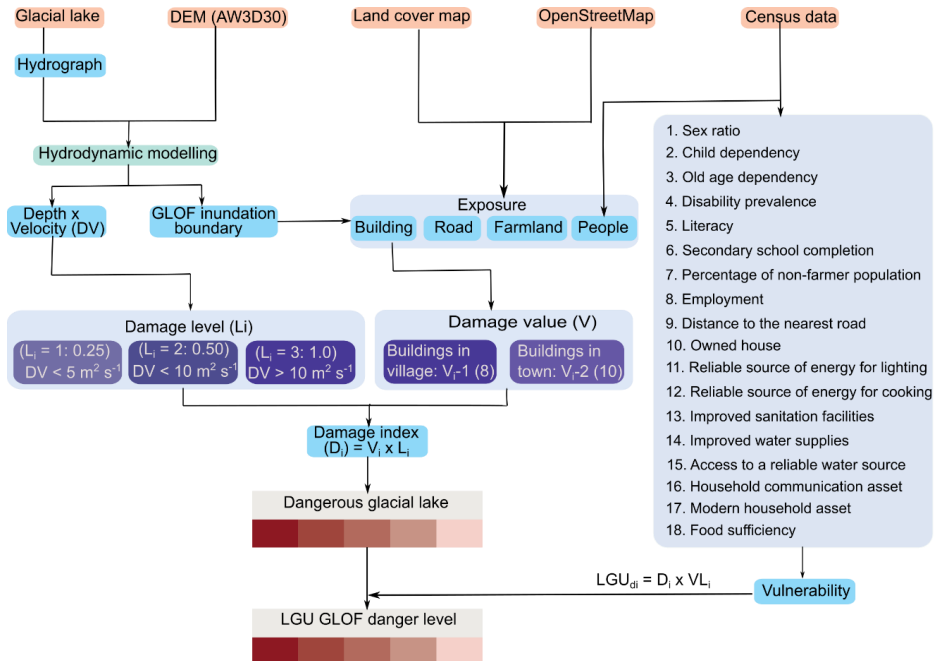


156 plants and two nearly commissioned hydropower plants (Punatsangchu-I and Punatsangchu-  
157 II) are located along these glacier-fed rivers (Fig.1). The agriculture sector, which is also  
158 heavily dependent on these river systems employs about 60% of the total population (786,385)  
159 (NSB, 2018). The built-up areas within the 1 km buffer of these glacier-fed rivers have  
160 increased by 200% (2.3 to 9.3 km<sup>2</sup>) within ~19 years from 2000 to 2019 (Fig.1) (Uddin et al.,  
161 2021). Thus, infrastructure and crucial economic activity have grown rapidly in areas  
162 downstream of glacial lakes in recent decades in Bhutan, making it vital to quantify the risk  
163 posed by GLOFs in these basins.

164 **3. Datasets and Methods**

165 **3.1. Lake dataset, drainage volume, peak discharge and flow hydrograph calculation**

166 We used the glacial lake inventory by Rinzin et al. (2021), which has been developed  
167 specifically for Bhutan, and which offers greater robustness and accuracy for Bhutan  
168 compared to the other datasets available at Pan-HMA scale (Zhang et al., 2023b; Zheng et  
169 al., 2021b). Rinzin et al. (2021) mapped 2,574 glacial lakes in 2020, located within 10 km of  
170 glacier termini and with a minimum lake area threshold of 0.003 km<sup>2</sup>. This dataset includes 85  
171 transboundary glacial lakes, located in the Indian and Chinese territories of Himalaya whose  
172 drainage flows into inland regions of Bhutan. Previous records indicate that GLOF originating  
173 from a relatively small lake (as small as 0.001 km<sup>2</sup>) can cause substantial damage in  
174 downstream communities, although such cases are rare. For instance, across HMA region,  
175 the median area of glacial lakes with known pre-outburst extents is approximately 0.189 km<sup>2</sup>  
176 (Shrestha et al., 2023). In Bhutan specifically, the smallest glacial lake with a documented  
177 outburst history has a present-day area of 0.0506 km<sup>2</sup> (Rinzin et al., 2021; Komori et al., 2012).  
178 Including all glacial lakes for detailed hydraulic modelling would substantially increase the  
179 computational demands, whereas resorting to simplified GIS-based approaches (Allen et al.,  
180 2019; Zheng et al., 2021b) to cover all lakes would significantly compromise the robustness  
181 and accuracy of the resulting of flood maps. Moreover, many smaller lakes are unlikely to  
182 generate significant downstream impacts unless they trigger secondary processes (Petrakov  
183 et al., 2020; Cook et al., 2018). Therefore, based on the above empirical evidence, and trade-  
184 off between model complexity and result reliability we focused on glacial lakes that (i) are at  
185 least 0.05 km<sup>2</sup> in area and (ii) are located within 1 km of glacier termini. This approach ensures  
186 a balance between computational feasibility and the production of reliable flood maps, while  
187 still capturing a substantial number of potentially hazardous lakes. Based on these criteria, we  
188 identified 278 glacial lakes in Bhutan for flood inundation mapping using hydrodynamic  
189 modelling (Fig. S1).



190

191 **Figure 2.** Flow chart showing an overview of the methodology we used for assessing GLOF  
192 danger in this study. Here GLOF damage index ( $D_i$ ) was calculated as the function of damage  
193 value ( $V_i$ ) and damage level ( $L_i$ ). The damage index for the local administrative unit ( $LGU_{di}$ ) is  
194 calculated by further multiplying with the vulnerability index ( $VL_i$ ). AW3D30 is abbreviated form  
195 for ALOS World 3D - 30m.

$$V = 42.95 \times A^{1.408}$$

(i)

Where  $V$  is the volume in  $10^6 \text{ m}^3$  and  $A$  is the area in  $\text{km}^2$

196 Accurate glacial lake volume data is crucial as one of the key determinants of modelled GLOF  
197 hydrodynamic characteristics such as flow depth and velocity. However, field based  
198 bathymetric measurement for multiple lakes is costly and not currently possible for some  
199 glacial lakes due to their remote location. In the absence of in-situ bathymetric data to  
200 determine volume, we calculated the volume of each glacial lake using the area-volume  
201 scaling relationship proposed by Zhang et al. (2023a) based on the area of each glacial lake  
202 as mapped in 2020 (Rinjin et al., 2021) (See table S1). This area-volume scaling relationship  
203 (equation (i)), based on recent bathymetric data from the Greater Himalayan region, including  
204 13 representative lakes from Bhutan is well-suited to approximate Bhutanese glacial lake  
205 volumes (Zhang et al., 2023a).



206 It is important to note that not all lakes drain entirely during a GLOF (Maurer et al., 2020; Nie  
207 et al., 2018; Zhang et al., 2024). However, previous data indicate smaller lakes are more likely  
208 to drain completely during a GLOF event than larger lakes. Here, we used data from Zhang et  
209 al. (2023b) documenting the drainage volumes of 64 lakes in the HMA regions. Among these  
210 64 lakes, the median percentage of drainage volume was 98% for lakes with an area < 0.1  
211 km<sup>2</sup>, 62% for lakes with an area of 0.1 to 1 km<sup>2</sup> and 33% for lakes with an area >1 km<sup>2</sup>. We  
212 used these observed drainage percentages as the basis to calculate the most likely flood  
213 volume generated by each lake. For simplicity and recognising that these median drainage  
214 values lie within the uncertainty bounds of established area-volume scaling relationships, we  
215 adopted the following assumptions: 100% drainage for lakes < 0.1 km<sup>2</sup>, 60% drainage for lakes  
216 between 0.1 and 1 km<sup>2</sup>, and 30% drainage for lakes > 1 km<sup>2</sup>. Subsequently, we used Evans's  
217 empirical equation (ii) for moraine-dammed lakes to calculate the possible peak discharge of  
218 each lake (Evans, 1986). See supplementary figure 1 (Fig. S1) for the distribution of volume  
219 and peak flow calculated for each glacial lake in Bhutan (see table S1).

$$Q_{max} = 0.72V^{0.53} \quad (ii)$$

$Q_{max}$  is peak discharge, and  $V$  is the total volume of the lake calculated using equation (i)

220 **3.2. HEC-RAS model set-up**

221 Most GLOFs start from moraine dam breaching, which is frequently triggered by large mass  
222 movement(s) entering the lake from the surrounding terrain hillslopes (Shrestha et al., 2023).  
223 However, conducting a dam breach simulation for each lake is challenging due to complexities  
224 and uncertainties in constraining the appropriate value for a large range of input parameters,  
225 (U.S. Army Corps of Engineers, 2021). To simplify this, we conducted a flood simulation  
226 resulting from each lake by using an input hydrograph as an upstream boundary condition.  
227 For each lake, we generated an input hydrograph by fitting the peak flow of each lake to the  
228 log-normal distribution curve with a standard deviation (sigma) value of 0.75 and a mean of 0,  
229 adapting the approach used by the earlier studies (Carr et al., 2024; Kropáček et al., 2015).  
230 For example, for lake1, the peak flow was 1,110 m<sup>3</sup> s<sup>-1</sup>, thus, we constructed a log-normally  
231 distributed hydrograph with a peak flow of 1,110 m<sup>3</sup> s<sup>-1</sup> and gradually decreased the flow after  
232 reaching this peak flow. With this assumption, we generated the hydrograph so that the flow  
233 rises to its peak rapidly and progressively decreases after attaining the peak, which is  
234 consistent with the hydrograph of many previous GLOF events (Maurer et al., 2020; Nie et al.,  
235 2020; Zheng et al., 2021a) (see supplementary figure S2 for representative hydrograph). The  
236 flow duration of the hydrograph of each lake was subsequently adjusted to account for  
237 the complete drainage of the estimated drainage volume calculated for each lake. For



238 example, for lake 1, the required drainage volume was calculated at  $1.036 \times 10^6 \text{ m}^3$  and so,  
239 the flow duration for this lake was adjusted so that the cumulative flow through the GLOF event  
240 was equal to this volume (Table S1).

241 We used the ALOS Global Digital Surface Model (AW3D30) with  $\sim 30 \text{ m}$  ground resolution as  
242 a source of terrain information for the model setup (Japan Aerospace Exploration Agency,  
243 2021). We chose AW3D30 because various previous studies (Rinzin et al., 2025) have  
244 indicated that it has higher vertical and horizontal accuracy compared to other freely available  
245 DEMs over our study area with similar spatial resolution such as SRTM GL1 (for example, Liu  
246 et al. (2019)). We assigned Manning's  $n$  value of 0.06 which is the default value in the HEC-  
247 RAS model set-up (U.S. Army Corps of Engineers, 2021) and has been used in GLOF  
248 modelling in Bhutan previously (Maurer et al., 2020).

249 We created one HEC-RAS project for each major river basin so that a total of seven project  
250 files correspond to the seven glaciated basins in Bhutan. For each project, the model domain  
251 was established by creating a 1,000 m buffer on either side of the centre line of the river  
252 originating from each lake. Within this model domain, a computational mesh with a grid  
253 resolution equal to the native resolution of AW3D30 ( $30 \times 30 \text{ m}$ ) was generated. An upstream  
254 boundary condition for each lake was defined at the frontal terminus of each lake. However,  
255 we used the same downstream boundary condition for all lakes in the basin, which were  
256 defined at the furthest end at the international border between Bhutan and India (for example,  
257 Fig. S2). Likewise, unique flow data was created for each lake, where we imposed flow  
258 hydrographs as the upstream boundary condition for the respective lake and downstream  
259 boundary conditions defined by normal depth with an energy slope of 0.01 (U.S. Army Corps  
260 of Engineers, 2021). Finally, one unsteady flow analysis plan for each lake with corresponding  
261 unsteady flow data and boundary conditions was developed. For example, in the Phochu  
262 basin, which contains 67 glacial lakes considered for this study, one project file was  
263 established. This project file included a single model domain, a downstream boundary  
264 condition, 67 upstream boundary conditions and 67 flow data. Accordingly, we created 67  
265 individual plans, each featuring the respective upstream boundary, uniform downstream  
266 boundary condition and flow data that contains the specific hydrograph for each lake (Fig. S2).

267 We computed all the simulations using the full momentum shallow water equations since it  
268 better represents GLOF rheology than the diffusion wave equation (Sattar et al., 2023; Sattar  
269 et al., 2021). Following the earlier studies (Rinzin et al., 2023; Maurer et al., 2020), all other  
270 computational parameters were maintained at the default setting. At a mesh size of 30 m, each  
271 model was run stably with a computational time step of 3 seconds within a courant number  
272 well below 2 (U.S. Army Corps of Engineers, 2021). The simulations were executed



273 simultaneously across 15 computers at the geospatial laboratory in Newcastle University. We  
274 maintained 10 hours of simulation time for each model set-up, which took 2 to 4 hours  
275 depending on the lake's size. Output for each project plan was carefully examined and any  
276 models exhibiting instability (e.g., a courant number above 2 or failed before complete  
277 execution) were re-executed by adjusting the position of upstream boundary condition,  
278 changing the timesteps and adding additional features like refinement regions within the 2D  
279 model domains to ensure stable model run and reliable results (U.S. Army Corps of Engineers,  
280 2021).

281 **3.3. GLOF impact area and exposed elements mapping**

282 We collated the GLOF inundation boundary for each lake generated through HEC-RAS  
283 modelling and calculated the area and length of each inundation. We calculated the population  
284 density per km<sup>2</sup> for each downstream local government administrative unit (LGU) using  
285 population data from the Bhutan 2017 population and census data (NSB, 2018), and from this  
286 population density map, we calculated the number of people exposed located GLOF  
287 inundation extent in each LGU. It is important to acknowledge that the population distribution  
288 data is simplified, although it is the most reliable dataset currently available for Bhutan. We  
289 mapped all buildings, roads, bridges, farmland, and hydropower plants within the GLOF  
290 inundation area to identify downstream elements at risk. We used OpenStreetMap (updated  
291 as of 30-04-2025) to map buildings, roads and bridges. We manually verified the  
292 OpenStreetMap data using Google Earth high-resolution imagery and updated 41 km of  
293 missing roads, 152 buildings and 20 bridges using Google Earth Imagery within the flood  
294 inundation plain. The ICIMOD's Landsat-based land use and landcover map of 2023 was used  
295 to map farmland (Uddin, 2021) since it is of better quality at the HKH scale than other open-  
296 access land cover data, such as Esri Sentinel-2 land cover data (Karra et al., 2021). We  
297 considered buildings the most important downstream exposed element because they are the  
298 primary space where people live mostly. Thus, we used exposed buildings to calculate the  
299 GLOF damage index (Fig. 2).

300 **3.4. GLOF damage and dangerous glacial lake calculation**

301 In this study, we defined a dangerous glacial lake based on the downstream damage  
302 (calculated here as damage index ( $D_i$ )) resulting from each GLOF event (Fig. 2). We assume  
303 that any of our study glacial lakes has the potential to generate GLOF in the future and the  
304 resulting damage will determine how dangerous that glacial lake would be to those  
305 downstream. The  $D_i$  for each element (pixel grid) resulting from any GLOF event was  
306 calculated as the function of the value of the exposed element ( $V_i$ ) and the level of damage  
307 ( $L_i$ ) following the approach proposed by Petrucci (2012) (equation (ii)) (Fig. 2). Qualitative data



308 such as construction type, occupancy, and value of the content of the building inside the house  
309 are essential to obtain the appropriate value of each element. However, such qualitative  
310 attributes are incomplete in the existing OpenStreetMap and introduce substantial  
311 uncertainties when estimated employing other open-access data. In this study, our focus is on  
312 providing a relative quantitative comparison of GLOF impacts across different communities  
313 instead of determining exact damage values resulting from each GLOF event. Thus, for  
314 simplicity, we assigned  $V_i$  of 8 to the buildings located in the rural areas and 10 to buildings  
315 located in the town areas, following the approaches used by Petrucci (2012) and Carrivick and  
316 Tweed (2016). The categorization of downstream communities into town and rural areas was  
317 achieved by using the local government administrative unit (LGU) map (Fig. 2).

$$D_i = V_i \times L_i \quad (\text{iii})$$

Where  $D_i$  is damage for each downstream exposed element,  $V_i$  is the value of each downstream element and  $L_i$  is the damage level for each element.

318 GLOFs with higher water flow velocity can cause more damage to the downstream elements  
319 than slow-flowing water (Federal Emergency Management Agency, 2004). Therefore, we  
320 calculated the  $L_i$  associated with each GLOF event as a function of both velocity and depth,  
321 which was accomplished by calculating the depth  $\times$  velocity ( $DV$ ) from the HEC-RAS output  
322 layer. The Federal Emergency Management Agency (FEMA) of the United States has  
323 established specific depth and velocity thresholds for assessing the collapse potential of  
324 buildings (Federal Emergency Management Agency, 2004). For instance, a one-story wood  
325 building is considered at risk of collapse if subjected to a flood depth of 3 m and a velocity of  
326  $1.6 \text{ m s}^{-1}$ . Applying these thresholds to this study is not appropriate for two key reasons: (1)  
327 the buildings in our study were not classified based on qualitative data such as construction  
328 material or type, and (2) these thresholds may not be directly applicable to the Bhutanese  
329 context, due differences in building design and construction. However, recognizing that higher  
330  $DV$  values correspond to greater damage levels, we categorized the  $DV$  values into three  
331 ranges corresponding to three levels of damage: Level 1:  $0-5 \text{ m}^2 \text{ s}^{-1}$  ( $L_i = 0.25$ ), Level 2:  $5-10$   
332  $\text{m}^2 \text{ s}^{-1}$  ( $L_i = 0.5$ ), and Level 3:  $>10 \text{ m}^2 \text{ s}^{-1}$  ( $L_i = 1$ ) (Fig. 2).

333 Finally,  $D_i$  of all damaged grid cell values within the GLOF path were summed to derive an  
334 overall damage value associated with GLOF from each lake (equation (iv)). This damage value  
335 was then normalized and ranked to classify the relative potential GLOF danger for each lake.

$$G_i = \sum D_i \quad (\text{iv})$$

$G_i$  is the geographical unit considered here: LGU and dzongkhag. When  $D_i$  for a lake was  
considered, the inundation boundary was considered for  $G_i$



336 **Table 1.** Socio-economic indicators used to calculate LGU's vulnerability to the future GLOF.  
337 The indicators were extracted from Bhutan's 2017 population and housing census. Details on  
338 how data for each indicator are collected are in National Statistics Bureau of Bhutan (2018).  
339 The calculated values were inverted so that they contribute positively to vulnerability for the  
340 indicators other than child dependency, old age dependency, and disability prevalence rate.

Indicator	Definition
Sex ratio	Number of males to every 100 females
Child dependency	The ratio of the number of children aged 0 to 14 years to population aged 15 to 64
Old age dependency	The ratio of persons 65 years and above to the population aged 15 to 64 years
Disability prevalence	The proportion of the population with a disability
Literacy	The ratio of the literate population (read and write in Dzongkha and English) aged 6 years and above to the total population of the same age group
Secondary school completion	The ratio of persons aged 6 years and above who have completed secondary education (grade XII) to the population of the same age group expressed in percentage
Percentage of non-farmer population	Percentage of people aged 15 years who are employed in sectors other than farming
Employment	Rate of persons aged 15 years and above who are employed
Distance to the nearest road	Households within the 30-minute walk to the nearest road point
Owned house	Household living in the owned house
Reliable source of energy for lighting	Households with a main source of energy for lighting as electricity
Reliable source of energy for cooking	Households with a main source of energy for cooking as electricity
Improved sanitation facilities	Households with improved sanitation facilities
Improved water supplies	Households with water supplies inside the dwelling
Access to a reliable water source	Households with availability of water supplies at least during the critical time (5 AM-8 AM, 11 AM - 2 PM and 5 PM-9 PM) adequate for washing and cooking
Household communication asset	Number of communication and media facilities owned by the individual households
Modern household asset	Number of modern household assets owned by individual households
Food sufficiency	Household having sufficient food to feed all the household members during the last 12 months

341 **3.5. Downstream community GLOF damage and danger mapping**

342 We conducted GLOF damage assessment for downstream settlements at various  
343 geographical scales: 20 districts and 274 local government administrative units (LGUs)  
344 (including 205 gewogs and 69 towns). We aggregated the  $D_i$  of each damage grid located  
345 within the respective LGU boundary to calculate the GLOF damage for each LGU using



346 equation (iv). In cases where downstream elements were affected by GLOFs originating from  
347 multiple lakes, the combined  $D_i$  from each contributing lake was considered in the analysis to  
348 account for their exposure to multiple possible GLOF hazards (Fig. 2).

349 As well as the magnitude of GLOF and the presence of downstream elements along the flow  
350 path, downstream GLOF damage is also determined by the community's capacity to prepare,  
351 respond and recover from a GLOF event (Cutter et al., 2008; Zhou et al., 2009). Lack of this  
352 capacity, often referred to as vulnerability, is influenced by wide-ranging socio-economic  
353 factors including but not limited to the standard of living and gender composition of the  
354 community (Cutter and Finch, 2008). Across the world, developed countries were found to be  
355 more disaster resilient than developing countries while disaster related death and damage  
356 have largely spiked in low-income countries (Rahmani et al., 2022). However, identifying  
357 specific socio-economic variables that are most relevant to GLOF damage remains a  
358 significant challenge, particularly because social data from past events are either unknown or  
359 at times overlooked. Past studies have used variables such as gross domestic product,  
360 population density (Carrivick and Tweed, 2016), human development index, corruption index  
361 and social vulnerability index at the national scale (Taylor et al., 2023a). While such data  
362 represent a broad overview of the country's socio-economic condition and thus vulnerability  
363 to disaster, they do not represent the regional and community level disparity within the country  
364 that influences their ability to respond and recover from the disaster. To address this, drawing  
365 upon our local understanding and following earlier studies (Allen et al., 2016; Rinzin et al.,  
366 2023), we calculated the relative vulnerability index ( $VL_i$ ) using a total of 18 socio-economic  
367 indicators from the 2017 Bhutan population and housing census NSB, 2018) (Table 1). This  
368 census data which is updated every after 10 years represents the most comprehensive and  
369 detailed dataset currently available, offering spatial granularity at the individual LGU level.  
370 These indicators are essential for evaluating a community's preparedness and response  
371 capacity to disaster from hazards like GLOF (Cutter and Finch, 2008). For example, Bhutan's  
372 traditionally gendered societal structure, men often assume more prominent roles in disaster  
373 response efforts. The  $VL_i$  for each LGU was calculated as the normalised value across these  
374 18 socio-economic indicators (Fig. 2). The definition and approach used for calculating each  
375 indicator is summarized in Table 1.

376 Assuming that the LGUs with higher  $VL_i$  are the least capable to respond to and recover from  
377 a future GLOF, the damage index ( $D_i$ ) of GLOF for each LGU unit was multiplied with to the  
378  $VL_i$  using equation (v).

$$LGU_{di} = D_i \times VL_i \quad (v)$$



Where  $LGU_{di}$  is the GLOF damage index for the individual LGUs normalized to their vulnerability index ( $VL_i$ )

379 **3.6. GLOF arrival time and GLOF monitoring assessment**

380 Building damage from GLOF is a function of hydrodynamic factors such as depth and velocity.  
381 On the other hand, human casualties and injuries also depend on the warning / response time,  
382 making it essential to consider flood arrival time in GLOF danger assessment. Thus, GLOF  
383 arrival time needs to be considered separately from the  $D_i$  we computed earlier. Accordingly,  
384 we determined the flow arrival time of the earliest arriving GLOF for each LGU to quantify the  
385 worst-case scenario for LGU exposed to multiple GLOF sourcing lakes.

386 The National Centre for Hydrology and Meteorology (NCHM), Bhutan monitor several lakes in  
387 Bhutan identified as dangerous (NCHM, 2019). Currently they have GLOF early warning  
388 system covering, Punatsangchu, Mangdechu and Chamkharchu basins which consists of 23  
389 monitoring stations (Fig. 1). We utilized monitoring station location data from NCHM to  
390 evaluate the relationship between Bhutan's existing early warning system, modelled GLOF  
391 scenarios originating from these glacial lakes and affected downstream communities. To  
392 achieve this, we first located all monitoring stations in Bhutan and counted how many of our  
393 catalogues of possible GLOFs in the region are covered by the existing early warning system  
394 based on their hydrological relationship (National Centre for Hydrology and Meteorology,  
395 2021). We assumed that if a GLOF flow intersects any of the existing EWS monitoring station,  
396 then the event considered to be monitored by the existing EWS in Bhutan. Similarly, if a LGU  
397 is affected by a GLOF that passes through one or more of these stations, the associated GLOF  
398 danger that LGU is regarded as being monitored by the existing EWS.

399 **Table 2.** GLOF exposed elements: people, buildings, roads, bridges and farmland distributed  
400 across top 20 GLOF LGUs. The total value at end last row represents the total exposed  
401 elements across all LGUs in Bhutan.

Gewog/town	District name	Building (count)	People count	Road (km)	Farmland (km <sup>2</sup> )	Bridge (count)	Danger (rank)
Chhoekhor	Bumthang	191	297	41.7	0.28	36	1
Bumthang Town	Bumthang	283	5740	13.3	2.32	2	2
Punakha Town	Punakha	272	4911	10.8	1.14	4	3
Lunana	Gasa	121	86	40.0	0.00	30	4
Toedwang	Punakha	60	86	5.0	1.08	8	5
Nubi	Trongsa	29	229	2.0	0.30	8	6
Thedtsho	Wangdue Phodrang	165	535	3.6	0.90	6	7



Dzomi	Punakha	53	560	6.2	1.22	6	8
Paro Town	Paro	262	5535	13.2	1.14	12	9
Wangdue Phodrang Town	Wangdue Phodrang	109	1365	1.2	0.25	0	10
Lamgong	Paro	195	303	7.9	0.85	6	11
Lingmukha	Punakha	65	41	5.7	0.19	2	12
Khoma	Lhuentse	42	49	6.7	0.04	8	13
Khatoed	Gasa	17	3	0.4	0.00	4	14
Athang	Wangdue Phodrang	38	3	2.0	0.42	10	15
Darkar	Wangdue Phodrang	85	21	3.2	0.31	16	16
Yalang	Yangtse	9	80	0.9	0.46	6	17
Langthil	Trongsa	11	44	1.3	0.82	8	18
Saephu	Wangdue Phodrang	6	162	14.2	0.00	4	19
Sharpa	Paro	120	168	3.8	0.94	8	20
<b>Total</b>		<b>2613</b>	<b>22399</b>	<b>265</b>	<b>19</b>	<b>364</b>	

402 **4. Results**

403 **4.1. GLOF impact and exposure**

404 Our study revealed that GLOFs from individual glacial lakes can travel as far as 167 km  
405 downstream and can inundate a maximum area of 30 km<sup>2</sup>. The modelled GLOFs exhibit a  
406 median travel distance of 40 km and an inundation area of 2.9 km<sup>2</sup> (Fig. S3). Collectively about  
407 2% (781 km<sup>2</sup>) of Bhutan's total land area is exposed to GLOF. The mean flow depth and  
408 velocity were 3.3 m and 3.4 m s<sup>-1</sup>, respectively (Fig. S3). The shortest arrival time to the  
409 nearest building was 8 minutes and the longest was 10 hours (Fig. S3). As a result, a total of  
410 22399 people, 2613 buildings, 270 km of road, 402 bridges, 19 km<sup>2</sup> of farmland and 4  
411 hydropower dams are exposed to GLOFs in Bhutan (Table 2). Of the total modelled GLOF  
412 events, 71% (n = 197) affect roads, 42% (n=116) affect buildings and 28% (n=77) affect  
413 farmland. The rest of the GLOFs do not affect any downstream entities. Focusing on Bhutan's  
414 most dangerous lake, Thorthormi Tsho, can impact 1119 buildings, 72 km of roads, and 4.2  
415 km<sup>2</sup> of farmland making it the most consequential event for reaching elements at risk. It is  
416 followed by lake278, located in the Wangchu basin and Chubdha Tsho in the Chamkharchu  
417 basin, both which are classified as high danger glacial lakes by this study (Table S1).

418 Out of 278 glacial lakes selected for flood mapping for this study, 85 (30.6%) are within  
419 catchments that cross the boundaries of India and China and drains into Bhutan inland. GLOF  
420 from these transboundary lakes also affect substantial number of downstream elements

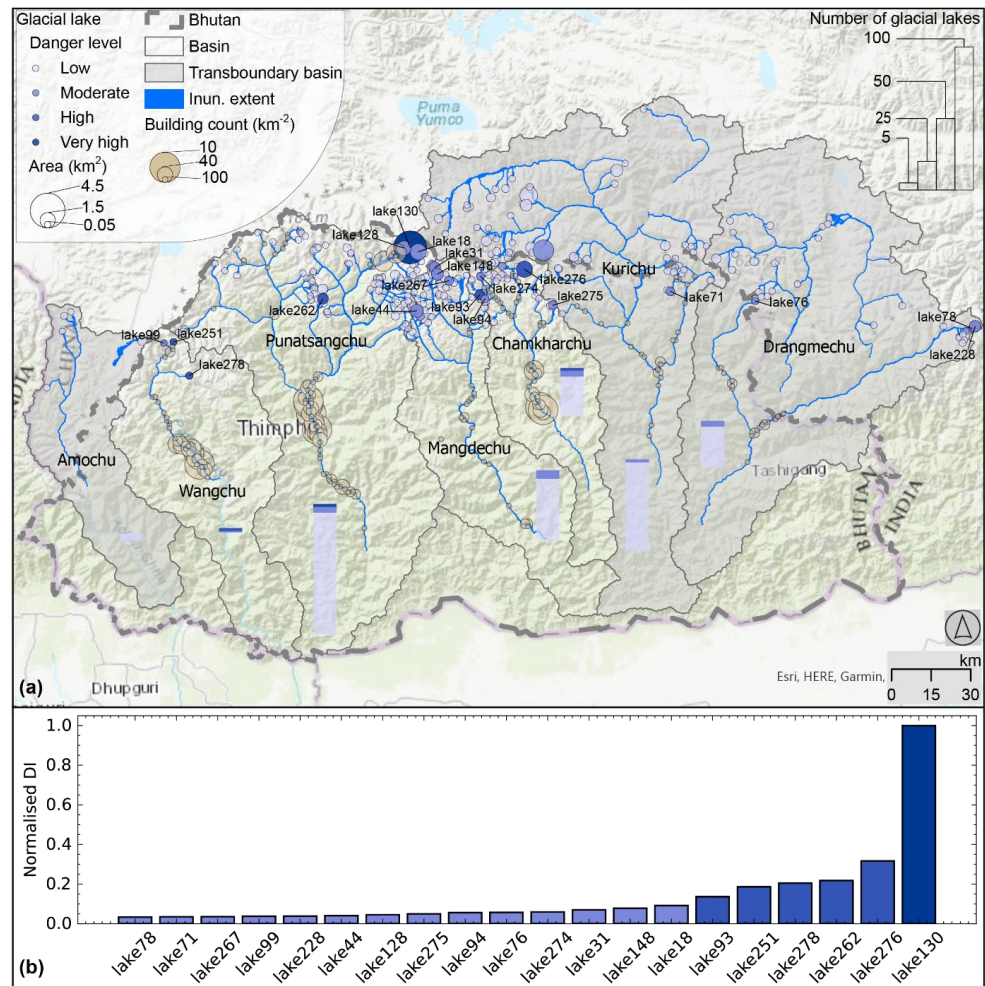


421 located in Bhutan, including 20 buildings, 0.6 km<sup>2</sup> of farmland, and 2 km of roads in Bhutan.  
422 All these exposed elements are situated within the Kurichu and Drangmechu basins.

423 The exposed elements are distributed across 17 districts and 88 local government  
424 administrative units (LGUs). Bumthang, Paro, Punakha, Wangdue Phodrang and Gasa  
425 districts are most affected by the GLOFs. For example, Paro itself has 673 GLOF exposed  
426 buildings, 32 km of road and 64 bridges (Table 2). Among the LGUs, the maximum exposed  
427 building is in Bumthang town (n= 283) followed by Punakha town (n= 272) and Paro town  
428 (n=262). The greatest road (roads, footpaths, tracks) inundation occurs in Chhoekhor followed  
429 by Lunana and Saephu, while most farmland is impacted in LGUs such as Bumthang town  
430 (2.3 km<sup>2</sup>), Dzomi Gewog (1.2 km<sup>2</sup>) and Paro town (1.1 km<sup>2</sup>) (Table S2).

431 **4.2. Dangerous glacial lakes**

432 We defined dangerous glacial lakes in Bhutan based on the damage index ( $D_i$ ) calculated by  
433 combining flow depth, velocity and downstream exposure data. Of the total lakes studied here  
434 (278), 164 had zero damage index as the GLOF from these lakes does not impact any  
435 buildings. The computed DI for rest of the glacial lakes range between 2 and 3435. Here we  
436 normalized DI value between 0 and 1. With the highest  $D_i$ , Thorthormi Tsho in the  
437 Punatsangchu basin emerged as the most dangerous high danger lake in Bhutan (Fig. 3).  
438 Additionally, based on DI, we categorized glacial lakes into four danger levels: very high  
439 danger, high danger, moderate danger, and low danger using the Natural Jenks classification  
440 system in ArcGIS. Using this approach, five other lakes are identified as high danger which  
441 are distributed across the Wangchu (2), Chamkharchu (2), and Punatsangchu (1) basins.  
442 Twenty-one of the glacial lakes were in the moderate danger category: four each in  
443 Punatsangchu, Chamkharchu and Drangmechu basins, and six in Mangdechu, two in Kurichu  
444 and one in Drangmechu basins (Fig. 3). The remaining (251) were classified as low danger.  
445 None of the high or very high danger glacial lakes were located within the Chinese and Indian  
446 sides of the basins, which drain into Bhutan (Fig. 3).



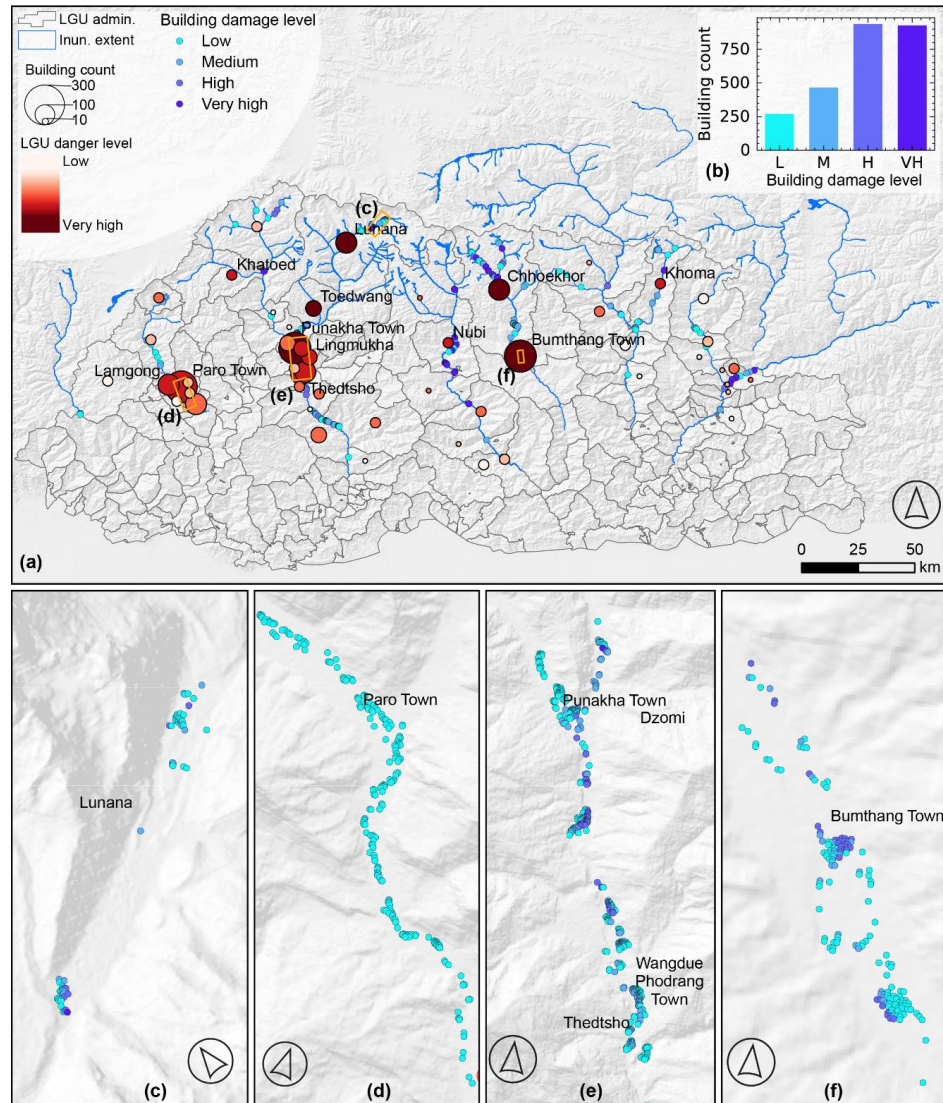
447

448 **Figure 3. Distribution of dangerous glacial lake.** The (a) map shows the distribution of  
449 glacial lake with associated GLOF danger level across the eight glaciated basins in Bhutan:  
450 very high (VH), high (H), moderate (M) and low dangers. The bar charts within the map show  
451 the number of glacial lakes (where height of the bar corresponds to number of lakes in each  
452 basin referenced to inset bar chart) with various danger levels in each basin. The bubble along  
453 the flood path shows number of buildings per  $\text{km}^2$ . The (b) bar chart shows the damage index  
454 (normalized between 0 to 1) associated with top 20 lakes arranged in the ascending order (left  
455 to right). The lake ID on the x-tick labels correspond to the ID on the map. Base map image is  
456 the intellectual property of Esri and is used herein under license. Copyright © 2025 Esri and  
457 its licensors. All rights reserved.



#### 458 4.3. Downstream GLOF danger

459 In this section, we present the GLOF damage ranking and level associated with downstream  
460 communities, encompassing 20 districts and 274 LGUs. Based on the damage index for  
461 respective LGUs ( $LGU_{di}$ ), which accounts for both damage from GLOF and people's  
462 vulnerability (Fig. S4), Punakha is identified as the district that would suffer from the highest  
463 GLOF damage in the future followed by Bumthang and Wangdue Phodrang districts.



464

465 **Figure 4.** Downstream GLOF danger. GLOF danger level across (a) local administration units  
466 and GLOF inundation extent (inun. extent). Inset (b) bar graph shows the number of all



467 buildings in Bhutan impacted by the modelled GLOF and associated damage level: very high  
468 (VH), high (H), moderate (M) and low (L). The lower panels (c–f) are the zoomed-in map from  
469 panel A which shows the damage level associated with individual buildings.

470 Among the LGUs, Chhoekhor gewog is associated with the highest GLOF damage followed  
471 by Bumthang town, Punakha town and Lunana gewog (Fig. 4). The classification of  $LGU_{di}$   
472 yielded five LGUs associated with very high GLOF damage while nine others were associated  
473 with high GLOF damage. Likewise, 13 LGUs were associated with moderate GLOF damage  
474 while the rest were identified as low GLOF damage LGUs (Fig. 4).

#### 475 **4.4. Flow arrival time**

476 We also ranked the LGUs based on the flow arrival time of the GLOF scenario that would  
477 impact the first buildings in the LGU. Results showed that, for the seven gewogs including  
478 Soe, Khoma, Chhoekhor, Lunana, Laya, Saephu, and Kurtoed, the fastest GLOF can impact  
479 some of their buildings within 30 minutes. Some buildings in Khatoed, Tsento, Toedwang and  
480 Nubi could be affected within one hour. Nine gewogs can be affected within 2 to 4 hours,  
481 another nine within 4–6 hours while the fastest GLOF could take more than 6 hours to affect  
482 buildings in other LGUs (Fig. 5).

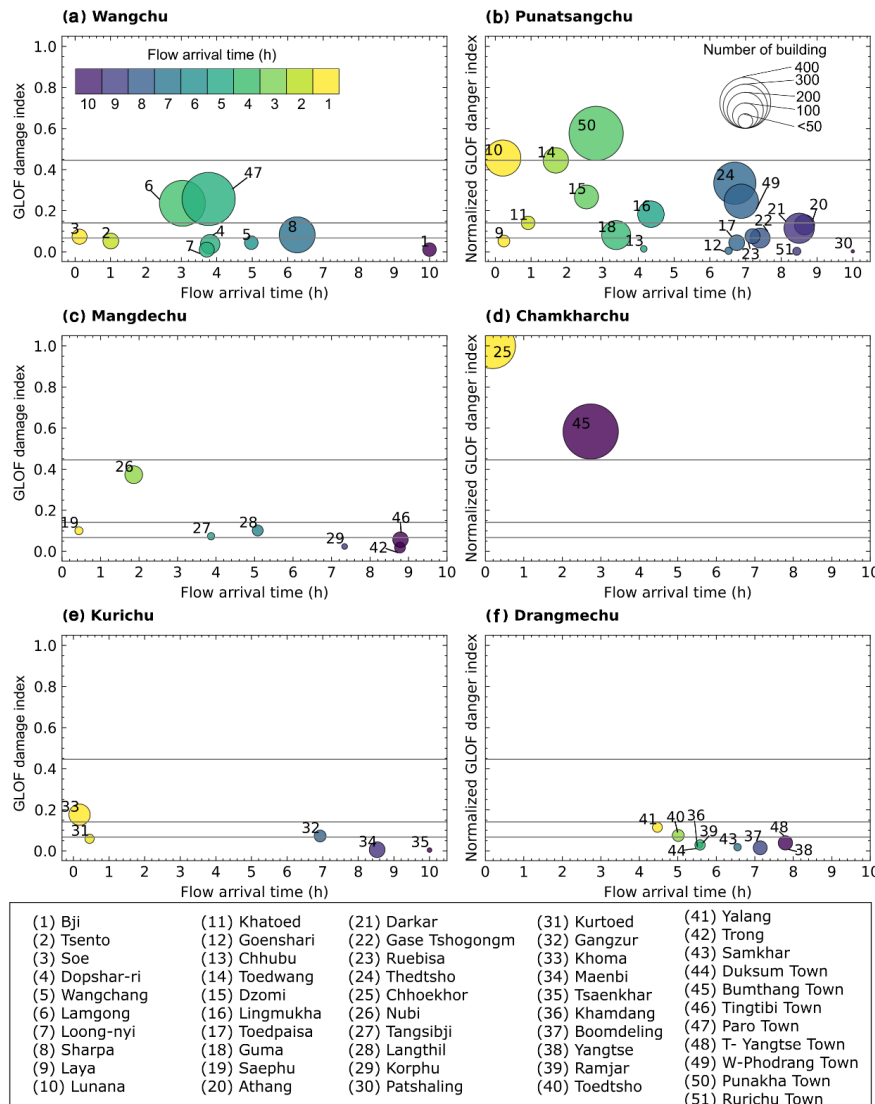
483 In the LGUs such as Soe and Laya, the first buildings affected by the GLOF are typically  
484 isolated and located very close to glacial lakes. Despite their proximity, the GLOF danger  
485 ranking for these LGUs remains relatively low due to the limited number of exposed buildings  
486 in these LGUs (Fig. 5). Therefore, we compared the  $Di$  and the arrival time of the fastest-  
487 arriving GLOF within each LGU. This analysis identified Lunana and Chhoekhor as LGUs with  
488 very high GLOF danger levels, and the fastest GLOF can arrive in as little as 15 minutes. On  
489 other hand, the fastest GLOF impacting buildings take up to three hours for other LGUs with  
490 very high GLOF danger such as Punakha town and Bumthang town (Fig. 5).

#### 491 **4.5 Early Warning System and GLOF**

492 We analyzed the distribution of the existing GLOF early warning system in Bhutan with respect  
493 to dangerous glacial lakes, and downstream communities associated with GLOF danger.  
494 Currently Bhutan has GLOF early warning system in three basins: Punatsangchu,  
495 Mangdechu, and Chamkharchu. Across these basins, the system is equipped with 13  
496 monitoring stations placed at various locations (Fig. 1). Assuming that GLOFs from a lake may  
497 be monitored if an EWS monitoring stations is located downstream of the glacial lake, our  
498 study shows existing EWS currently tracks 51 out of the 278 glacial lakes we investigated  
499 here. Among these monitored lakes, the network includes the most dangerous glacial lake,  
500 Thorthormi Tsho, as well as two of the five high danger glacial lakes and five of the six



501 moderate danger glacial lakes. The remaining monitored lakes are classified as low or very  
 502 low danger. Notably the high danger glacial lakes identified here including lake251, lake262  
 503 and lake278 are not monitored by the existing early warning systems.

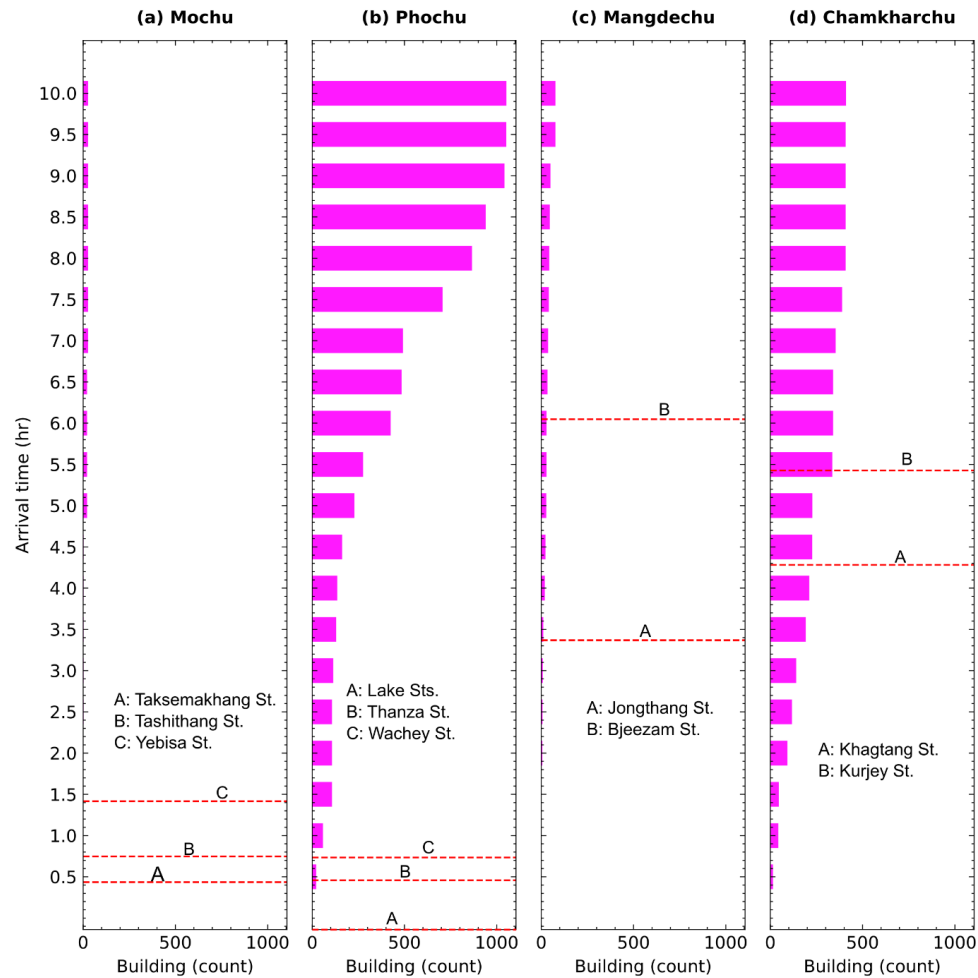


504

505 **Figure 5.** The damage index and flow arrival time (of the fastest arriving) GLOF for each local  
 506 administrative unit (LGUs) in impacted basins: (a) Wangchu, (b) Punatsangchu, (c)  
 507 Mangdechu, (d) Chamkarchhu, (e) Kurichu and (f) Drangmechu. Numbers associated with  
 508 each bubble in plot correspond to the numbering corresponding to the name of each LGU in  
 509 the lower panel. The flow arrival time colour code legend in panel (a) and number of building



510 legend in panel (b) applies to all the panels. The horizontal grey lines categorize the local  
511 administrative unit (LGUs) into various GLOF danger level based on damage index (low  
512 danger level to very high danger level).



513  
514 **Figure 6.** Bar plots showing the number of buildings located downstream of GLOF early  
515 warning monitoring stations in Punatsangchu basin [(a) Mochu, (b) Phochu], (c) Mangdechu,  
516 and (d) Chamkharchu basins. Red dashed lines represent the location of EWS monitoring  
517 stations relative to average flow arrival time of all GLOFs detected by each EWS monitoring  
518 station. The bars represent cumulative numbers of GLOF exposed buildings located at the  
519 respective basin where early warning stations are operational. The name location of each  
520 EWS monitoring station is indicated with alphabet (A to C) within the respective panel. The



521 monitoring station located at the lakes including Bechung, Raphstreg, Thorthormi and Lugge  
522 Tsho in Phochu basin are marked as Lake Sts. in panel (b).

523 We further examined residents of how many GLOF exposed buildings can receive early  
524 warnings based on their hydrological relationship to the existing EWS monitoring stations.  
525 Assuming that the buildings located downstream of the EWS monitoring stations can receive  
526 early warning, our study revealed that the existing GLOF monitoring stations can provide early  
527 warning to the people living in 1549 buildings of which about 75% are in the Punatsangchu  
528 basin. Of these, residents in 268 buildings are estimated to have less than 30 minutes to  
529 evacuate after receiving warning from the EWS monitoring stations located in their respective  
530 communities (Fig. 6).

531 Conversely, people living in 1050 exposed buildings, that is at least 41% of them do not have  
532 access to early warning coverage. Approximately half of these unserved buildings clustered  
533 in downstream LGUs with high GLOF danger including Lamgong and Paro Town in Paro  
534 districts. Although EWS in place in the Chamkharchu basin, a cluster of about 82 buildings in  
535 Chhoekhor in Bumthang are not covered by EWS. These is because the flood waves from the  
536 potential GLOF can arrive these buildings before activating the monitoring stations at  
537 Khagtang and Kurjey (Fig. 6).

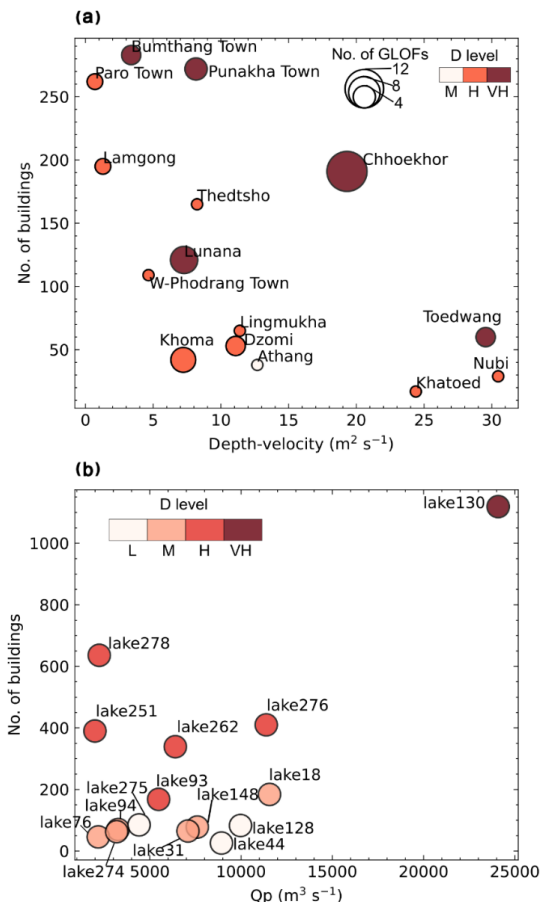
538 **5. Discussion**

539 **5.1. Redefined dangerous glacial lake**

540 Some of the most devastating historical GLOF events in the world have occurred from  
541 seemingly inconspicuous glacial lakes (Allen et al., 2015; Petrakov et al., 2020), whilst some  
542 large-magnitude GLOF events have caused minimal or no downstream damage (Shrestha et  
543 al., 2023; Lützow et al., 2023). This is because the GLOF magnitude alone does not determine  
544 downstream damage caused by the GLOF event, instead, it is the interaction between GLOF  
545 magnitude and the downstream exposed elements that determine the extent of damage  
546 (Taylor et al., 2023a). For example, the greatest structural damage associated with 2023 South  
547 Lhoknak Lake GLOF event in the Indian state of Sikkim occurred between 200 and 385 km  
548 downstream of the glacial lake, with 59% of these impacted structures constructed within the  
549 past decade (Sattar et al., 2025). This highlights the escalating risks posed by infrastructure  
550 expansion and settlement growth in GLOF-exposed areas and underscores the importance of  
551 considering exposure data in GLOF danger assessment. To address this in Bhutan, we  
552 redefined dangerous glacial lakes by coupling flood characteristic modelling and downstream  
553 exposure data. Accordingly, we have produced flood mapping and GLOF danger ranking for  
554 278 glacial lakes along with comprehensive GLOF danger assessments for 274 local



555 government administrative units (LGUs). As a result, we classified lake130 (Thorthormi Tsho)  
556 as a very high danger glacial lake in Bhutan, five lakes (lake93, lake251, lake262, lake276  
557 and lake278) as high danger and 21 other lakes as moderate danger. Likewise, five  
558 downstream LGUs were associated with very high GLOF danger while nine others were  
559 associated with high GLOF danger.



560  
561 **Figure 7.** Dot plot illustrating the influence of GLOF magnitude and downstream exposure on  
562 danger level computed in this study for (a) downstream LGUs and (b) individual lakes. In panel  
563 (a), the GLOF magnitude is based on median depth-velocity across all the GLOFs that strike  
564 at least one building in the LGU. In panel (b), we considered peak discharge (Qp) as a proxy  
565 for GLOF magnitude. In both the panels, colour associated with each dot indicates the GLOF  
566 danger (d) level associated with each LGU or lake. The size of the dots in panel (a)  
567 corresponds to number of GLOFs from various glacial lakes that impact the respective



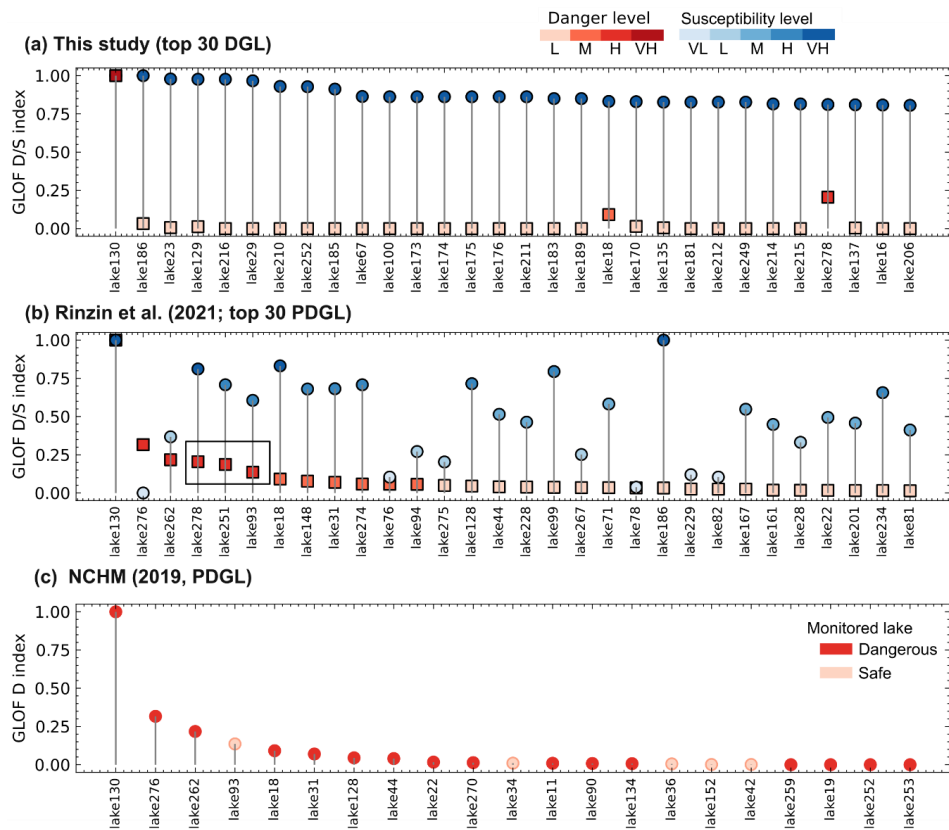
568 community. For the better visualization, only top 15 dangerous glacial lake and top 15 LGUs  
569 with GLOF danger are displayed here.

570 Our approach departs from many existing practices of identifying dangerous glacial lakes,  
571 which are primarily based on the susceptibility of lakes to produce GLOF without regarding  
572 the characteristics of settlements located downstream of the lakes (Rinzin et al., 2021; NCHM,  
573 2019), in two ways: **1) Incorporation of GLOF Hydrodynamic characteristics:** we  
574 considered flow velocity and flow depth, which are both primary components of the GLOF flow  
575 that determine damage to the downstream elements (Federal Emergency Management  
576 Agency, 2004). **2) Interaction of flow depth and velocity with downstream exposed**  
577 **buildings:** we mapped potential downstream building damage associated with each GLOF  
578 event based on the interaction between the depth-velocity and downstream at-risk elements.  
579 By focusing on the interaction between flood magnitude and downstream exposed building,  
580 our method classifies glacial lakes as dangerous only when their potential flood poses a threat  
581 to downstream elements, making it a more practical and effective strategy for bespoke GLOF  
582 risk reduction activities. For example, lake278 and lake251 are small and they produce  
583 relatively small GLOFs with their estimate peak discharge approximately  $2000 \text{ m}^3 \text{ s}^{-1}$ .  
584 However, both were classified as high danger as the GLOF from these lakes impact hundreds  
585 of downstream buildings (Fig. 7). Likewise, our approach assigns a higher GLOF danger  
586 ranking to communities that are either affected by GLOFs from multiple lakes, impacted by  
587 high-magnitude GLOFs, or have multiple buildings located within the GLOF inundation area,  
588 whilst also considering the community's vulnerability. For example, Chhoekhor was identified  
589 as having the highest GLOF danger in Bhutan because at least 191 buildings were potentially  
590 impacted by GLOF from as many as 14 lakes in the basin. On other hand, other gewogs such  
591 as Toedwang in Punakha also are classified as having very high GLOF danger, despite having  
592 a comparatively low number (60) of potentially impacted buildings because these building  
593 could be impacted by very high magnitude GLOFs in terms of depth and velocity (Fig. 7).

594 Our approach challenges traditional dangerous glacial lake assessments by redefining which  
595 glacial lakes pose the greatest danger to the downstream settlements. As a result, we  
596 identified three new high danger glacial lakes including, lake93 (Phudung Tsho), lake251, and  
597 lake278 (Wonney Tsho), which are not recognized as dangerous glacial lakes by any of the  
598 previous studies. Also, 53 of the previously identified 64 very highly susceptible to GLOFs  
599 lakes (Rinzin et al., 2021) are categorized as low GLOF danger lakes. Conversely, 12 lakes  
600 classified as low or very low GLOF susceptibility emerge as moderate to high danger in our  
601 study (Rinzin et al., 2021). Likewise, nine of the dangerous lakes monitored by NCHM (six in  
602 Punatsangchu basin, one each in Mangdechu, Chamkharchu and Kurichu basins) (National



603 Centre for Hydrology and Meteorology, 2019) are categorized as low danger in our study (Fig.  
604 8). These discrepancies arise because we classified lakes as dangerous only if a potential  
605 GLOF would affect a significant number of downstream buildings, whereas earlier studies  
606 relied solely on geomorphological characteristics of the lakes and their surroundings (Rinzin  
607 et al., 2021; NCHM, 2019) (Fig. 8). For example, lake278 in the Wangchu headwaters is  
608 classified as high danger in our study because a potential GLOF could impact 636 buildings  
609 across seven LGUs in Paro while the earlier studies considered this lake as safe as it does  
610 not have geomorphological characteristics and lake condition to qualify as dangerous (Rinzin  
611 et al., 2021).



612  
613 **Figure 8.** Comparison (a, b) GLOF damage index (DI) for top 30 dangerous glacial lakes  
614 (DGL) calculated in current study and GLOF susceptibility score from Rinzin et al. (2021), and  
615 (c) damage index (DI) for potentially dangerous glacial lakes (PDGLs) in Bhutan identified by  
616 National Centre for Hydrology and Meteorology (2019). The black bounding box in panel (b)  
617 shows the new dangerous glacial lakes identified in this study for the first time.



618 By ranking GLOF danger for all 274 LGUs, we discovered new GLOF risk hotspots such as  
619 Paro town and Lamgong gewog (Paro, Khoma gewog [Lhuentse] and Chhoekhor gewog  
620 [Bumthang]). GLOF danger in these places was previously not quantified and existing GLOF  
621 early warning systems in Bhutan currently do not cover these high GLOF danger LGUs  
622 (NCHM, 2021). We therefore recommend prioritizing monitoring of glacial lakes in Bhutan  
623 based on high downstream exposure, rather than focusing on lakes selected solely based on  
624 geomorphic susceptibility assessments. Specifically, Bhutan's glacial lake monitoring and  
625 downstream risk mitigation efforts should expand beyond Lunana to include other high GLOF  
626 danger lakes and vulnerable downstream settlement such as Paro Town, and Chhoekhor  
627 gewog and gradually expanding to currently understudied areas in far eastern districts such  
628 as Lhuentse, while emphasizing that higher granularity studies might be needed to guide  
629 bespoke risk reduction efforts in these respective areas.

630 **5.2. Transboundary GLOF**

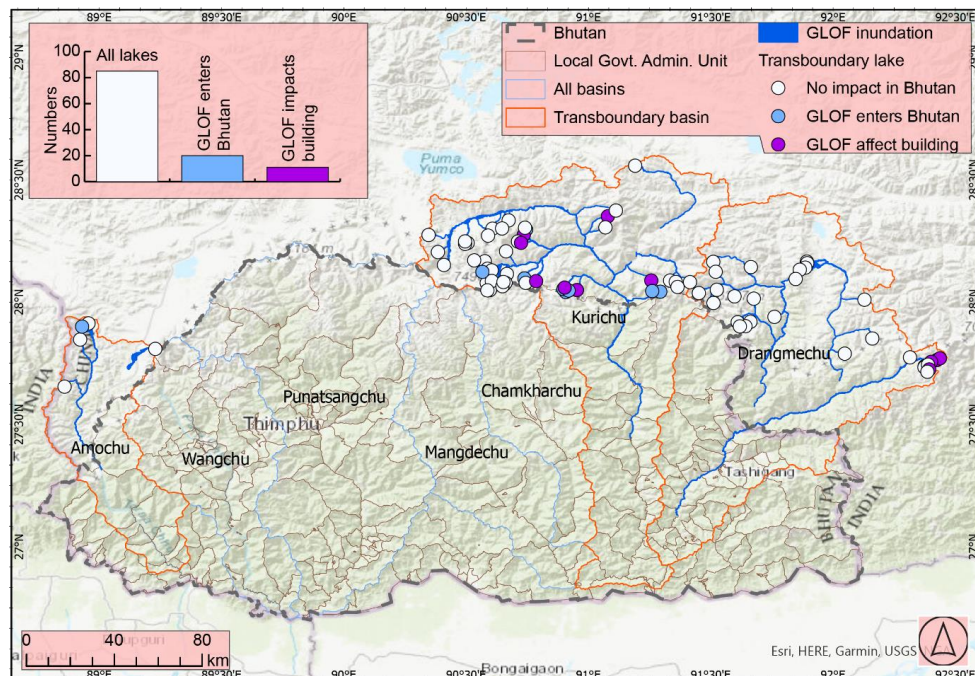
631 None of the transboundary lakes were classified as very high or high danger based on  
632 potential GLOF impacts in Bhutan. This is because damage was minimal, mainly inundating  
633 uninhabited parts of Bhutan, located in deep, inaccessible gorges. However, we identified  
634 GLOF from four lakes in the Drangmechu basin (located in Arunachal Pradesh, India) and 11  
635 in the Kurichu basin (located in the Tibetan Autonomous Region, China), which could  
636 potentially impact several buildings in Bhutan. Furthermore, GLOF from 20 lakes located in  
637 the Indian and Chinese territories of the Himalaya enter Bhutan, although they do not impact  
638 any building (Fig. 9). Identifying potential transboundary GLOFs is vital, given their potential  
639 destructive power and long run out distances and challenges stemming from absence of  
640 transboundary GLOF risk mitigation mechanism. For example, a recent GLOF from South  
641 Lhoknak Lake in the Indian Himalaya has travelled over 300 km downstream, causing  
642 significant damage in Bangladesh (Sattar et al., 2025). The absence of transboundary  
643 cooperation for GLOF risk mitigation between Bhutan, China, and India complicates efforts to  
644 monitor and manage such risks. Establishing regional cooperation is essential to enhance  
645 early warning systems, facilitate data sharing, and implement coordinated risk reduction  
646 strategies, thereby minimizing the potential damage from future transboundary GLOFs.

647 **5.3. Significance, limitations and the way forward**

648 Our approach of GLOF danger assessment using both flood magnitude and downstream  
649 exposure data provides local authorities and relevant stakeholders with valuable information  
650 to plan and prioritize wide ranging risk mitigation activities. These activities may target either  
651 specific glacial lakes or downstream communities based on the danger index and level we  
652 have provided, whilst also incorporating practical factors, such as resource availability and



653 logistical constraints. This study is particularly timely, as the Royal Government of Bhutan is  
654 planning to modernize and expand its network of flood monitoring and GLOF early warning  
655 systems (World Bank, 2024). This initiative, outlined in the roadmap for 2024–2034, aims to  
656 develop multi-hazard warning services, aligning closely with the practical applications and  
657 insights provided by our research. For example, our flood mapping and flow arrival time data  
658 can be used to appropriately locate GLOF monitoring stations for early warning systems  
659 (Wang et al., 2022). Likewise, some of the scattered buildings in LGUs such as Soe gewog in  
660 Paro could be impacted by GLOFs within as little as 10 minutes. This short lead time means  
661 it is practically not effective to install early warning systems for residents in these rapidly  
662 affected areas. In such context, our flood extent mapping can effectively guide land-use zoning  
663 and support informed decision-making for future development in these vulnerable locations.



664  
665 **Figure 9.** The map shows the impact of GLOF in Bhutan, which originates from lakes located  
666 on the Chinese and Indian sides of Transboundary basins. The inset bar graph shows the total  
667 lakes, lakes from which GLOF enters Bhutan and lakes from which GLOF impacts buildings  
668 and other structures in Bhutan. The lake ID on the x-tick labels correspond to the ID on the  
669 map. Base map image is the intellectual property of Esri and is used herein under license.  
670 Copyright © 2025 Esri and its licensors. All rights reserved.



671 Our work establishes a baseline GLOF mapping and risk assessment in Bhutan. However, we  
672 acknowledge that the magnitude of flood from glacial lakes will continue to evolve as glacier  
673 retreat drives the expansion of existing lakes within a topographically constrained extent and  
674 the formation of new lakes within the depressions left by the retreating glaciers (Zheng et al.,  
675 2021b; Furian et al., 2022). Concomitantly, the downstream settlements within the GLOF-  
676 prone areas are evolving, with population growth and infrastructure development leading to  
677 increased GLOF exposure. The interplay of these factors means GLOF danger will likely  
678 increase in the future and highlights the need for dynamic and regularly updated GLOF flood  
679 mapping and risk assessments in the future.

680 We determined the minimum glacial lake area threshold ( $0.05 \text{ km}^2$ ) for GLOF modelling based  
681 on the empirical evidence from the previous inventory (Shrestha et al., 2023; Komori et al.,  
682 2012). However, it is important to acknowledge that glacial lake smaller than  $0.05 \text{ km}^2$  have  
683 also been known to produce GLOF event with a magnitude substantial to cause significant  
684 downstream damage, particularly when it combines with other flood like meteorological flood  
685 (Allen et al., 2015) or when the outburst flow entrains large amount of debris (Petrakov et al.,  
686 2020; Cook et al., 2018). Thus, the future modelling effort should also consider smaller lakes  
687 than the size threshold we considered here.

688 While we mapped all types of exposed elements located within the GLOF flow inundation  
689 extent, our GLOF danger index is calculated solely based on the impact on number of exposed  
690 buildings. This approach is grounded in the rationale that buildings represent the primary  
691 places where people reside and are therefore the most direct proxy for population exposure.  
692 However, critical infrastructure such as hydropower plants (e.g., in the Punatsangchu basin)  
693 and the international airport in Paro (Wangchu basin), which are vital to the national economy,  
694 were not included in our danger calculation. This omission stems from the considerable  
695 challenges involved in accurately estimating the economic cost of potential damage to such  
696 high-value infrastructure. When the GLOF intercepts hydropower dams, it can cause  
697 overtopping, excessive sedimentation, outages, equipment damage leading to significant  
698 revenue losses from the hydropower plants (Dunning et al., 2006) as well as cascading  
699 impacts on the low-lying settlements (Sattar et al., 2025). Likewise, damage to the crucial  
700 infrastructure such as Paro international airport will hinder relief effort after the GLOF disaster  
701 delaying the recovery and escalating overall loss and damage. Therefore, future study should  
702 also consider absolute economic impact of GLOF to aid relevant stakeholders and  
703 policymakers in developing appropriate strategies to mitigate risks to vital infrastructure.

704 Looking forward, the glacial lake dataset can be updated using wide-ranging open-access  
705 remote sensing imagery. Similarly, platforms such as OpenStreetMap, which leverage crow-



706 sourced data and are frequently updated, present a valuable resource for mapping evolving  
707 downstream buildings and other structure data. Likewise, hydrodynamic modelling for multiple  
708 glacial lakes with freely available and user-friendly models such as HEC-RAS is increasingly  
709 becoming feasible with the recent development in artificial intelligence and cloud-based  
710 computing platforms like Flood Platform (<https://www.floodplatform.com/>) which enable  
711 integrating products from varied flood simulations/models into a common framework. We will  
712 develop web portal, which hosts glacial lake data and flood maps, serves as a valuable  
713 resource for periodic updates to flood damage assessments. By integrating up-to-date glacial  
714 lake flood magnitude information with evolving downstream exposure data, this platform can  
715 provide valuable information for informed decision-making and proactive risk management,  
716 such as tailored early warning systems and land use management and development.

717 **6. Conclusion**

718 Glacial lakes, which are growing in number and areas in the mountains globally, pose a serious  
719 GLOF threat to the communities living downstream of them. However, the destruction and  
720 damage caused during the GLOF events are not only a function of lake drainage magnitude  
721 but also depend on their interaction with downstream exposed elements. Despite this,  
722 traditional approaches to assessing danger posed by glacial lakes have been mainly based  
723 on the likelihood and magnitude of a lake to produce GLOFGLOF and often disregard the  
724 potential downstream impact. To address this gap, this study redefines the classification of  
725 dangerous glacial lakes in Bhutan (one of the high GLOF risk countries globally) by combining  
726 GLOF hydrodynamic characteristics mapping and downstream exposed buildings.

727 This study produced GLOF hydrodynamic characteristics for all glacial lakes in Bhutan which  
728 are greater than 0.05 km<sup>2</sup> and located within the 1 km of glacier terminus. The analysis  
729 revealed that approximately 22399 people, 2613 buildings, 270 km of road, 402 bridges and  
730 20 km<sup>2</sup> of farmland are exposed to GLOF in Bhutan. A GLOF damage index was developed  
731 by combining flood mapping data with downstream exposure metrics, enabling the ranking of  
732 glacial lakes based on their potential danger. Thorthormi Tsho was identified as the most  
733 dangerous glacial lakes in Bhutan. Furthermore, we identified five additional glacial lakes as  
734 having high GLOF danger, two of which are in head water of Wangchu, neither included in  
735 previous study and nor monitored by existing early warning system in Bhutan. Among these  
736 dangerous glacial lakes, three of them are newly identified dangerous glacial lakes (lake251,  
737 278 and lake93) in the current study.

738 For the first time, this study provides GLOF danger ranking for 20 districts and 274 local  
739 government administrative blocks (gewogs and towns) [LGUs] in Bhutan. In addition to the



740 previously identified high GLOF danger gewogs and towns, we have identified six additional  
741 LGUs with similarly high GLOF dangers. These include Chhoekhor and Bumthang town in  
742 Bumthang, Paro town and Lamgong in Paro, Nubi in Trongsa and Khoma in Lhuentse districts.

743 Most strikingly, some downstream LGUs such as Paro town and Lamgong gewog in Paro are  
744 not covered by the existing Bhutan early warning system, highlighting significant gaps in  
745 existing risk mitigation efforts.

746 This study underscores the criticality of incorporating flood mapping and downstream  
747 exposure and vulnerability data when defining GLOF dangerous lake and assessing  
748 downstream risk. For Bhutan, the findings emphasize the urgent need to expand and  
749 strengthen GLOF risk mitigation strategies, including the enhancement of early warning  
750 systems and the implementation of targeted interventions in newly identified high-risk areas.  
751 These measures are essential to safeguarding vulnerable communities and infrastructure from  
752 the escalating threat of GLOFs in the context of ongoing climate change and glacial retreat.

### 753 **Acknowledgement**

754 This work was supported by the Natural Environment Research Council (NERC)- funded  
755 IAPETUS Doctoral Training Partnership [IAP2-21-267].

### 756 **Code and data availability**

757 The HEC-RAS 2D model we used here for simulating glacial lake outburst modelling can be  
758 accessed at: <https://www.hec.usace.army.mil/>. The AW3D30 DEMS used here can be  
759 downloaded from the OpenTopography at: [OpenTopography - Find Topography Data](#). Bhutan  
760 2017 housing and census data can be downloaded from National Statistical Bureau of Bhutan  
761 at <https://www.nsb.gov.bt/>. Landover and landuse data used in this study can be accessed at:  
762 <https://rds.icimod.org/>. The OpenStreetMap data can be assessed at:  
763 <https://www.openstreetmap.org/relation/184629>. GLOF hydraulic data for each glacial lake will  
764 be made available through web portal with publishing of this article.

### 765 **Supplement**

766 The supplement related to this article is available online at:

### 767 **Author contributions**

768 SR, SD and RC conceptualized the study. SR undertook data analysis, visualization and wrote  
769 original draft. SD and RC secured the funding, supervised and contributed equally to the work.



770 SA, AS and SW reviewed and edited the manuscript. All authors contributed to the final  
771 manuscript.

772 **Competing interests**

773 The contact author has declared that none of the authors has any competing interests.

774



## 775 References

776 Allen, S., Frey, H., and Huggel, C.: Assessment of Glacier and Permafrost Hazards in Mountain Regions.  
777 Technical Guidance Document, 10.13140/RG.2.2.26332.90245, 2017.

778 Allen, S. K., Rastner, P., Arora, M., Huggel, C., and Stoffel, M.: Lake outburst and debris flow disaster at  
779 Kedarnath, June 2013: hydrometeorological triggering and topographic predisposition, *Landslides*, 13,  
780 1479-1491, 10.1007/s10346-015-0584-3, 2015.

781 Allen, S. K., Zhang, G., Wang, W., Yao, T., and Bolch, T.: Potentially dangerous glacial lakes across the  
782 Tibetan Plateau revealed using a large-scale automated assessment approach, *Science Bulletin*, 64,  
783 435-445, 10.1016/j.scib.2019.03.011, 2019.

784 Allen, S. K., Linsbauer, A., Randhawa, S. S., Huggel, C., Rana, P., and Kumari, A.: Glacial lake outburst  
785 flood risk in Himachal Pradesh, India: an integrative and anticipatory approach considering current and  
786 future threats, *Natural Hazards*, 84, 1741-1763, 10.1007/s11069-016-2511-x, 2016.

787 Byers, A. C., Rounce, D. R., Shugar, D. H., Lala, J. M., Byers, E. A., and Regmi, D.: A rockfall-induced  
788 glacial lake outburst flood, Upper Barun Valley, Nepal, *Landslides*, 16, 533-549, 10.1007/s10346-018-  
789 1079-9, 2018.

790 Carr, J. R., Barrett, A., Rinzin, S., and Taylor, C.: Step-change in supraglacial pond area on Tshojo Glacier,  
791 Bhutan, and potential downstream inundation patterns due to pond drainage events, *Journal of  
792 Glaciology*, 1-40, 10.1017/jog.2024.62, 2024.

793 Carrivick, J. L. and Tweed, F. S.: A global assessment of the societal impacts of glacier outburst floods,  
794 *Global and Planetary Change*, 144, 1-16, 10.1016/j.gloplacha.2016.07.001, 2016.

795 Colavitto, B., Allen, S., Winocur, D., Dussaillant, A., Guillet, S., Munoz-Torero Manchado, A., Gorsic, S.,  
796 and Stoffel, M.: A glacial lake outburst floods hazard assessment in the Patagonian Andes combining  
797 inventory data and case-studies, *Sci Total Environ*, 916, 169703, 10.1016/j.scitotenv.2023.169703,  
798 2024.

799 Cook, K. L., Andermann, C., Gimbert, F., Adhikari, B. R., and Hovius, N.: Glacial lake outburst floods as  
800 drivers of fluvial erosion in the Himalaya, *Science*, 362, 53-57, doi:10.1126/science.aat4981, 2018.

801 Cook, S. J., Kougkoulos, I., Edwards, L. A., Dorch, J., and Hoffmann, D.: Glacier change and glacial lake  
802 outburst flood risk in the Bolivian Andes, *The Cryosphere*, 10, 2399-2413, 10.5194/tc-10-2399-2016,  
803 2016.

804 Cutter, S. L. and Finch, C.: Temporal and spatial changes in social vulnerability to natural hazards, 105,  
805 2301-2306, 10.1073/pnas.0710375105 %J Proceedings of the National Academy of Sciences, 2008.

806 Cutter, S. L., Barnes, L., Berry, M., Burton, C., Evans, E., Tate, E., and Webb, J.: A place-based model for  
807 understanding community resilience to natural disasters, *Global Environmental Change*, 18, 598-606,  
808 10.1016/j.gloenvcha.2008.07.013, 2008.

809 Das, S., Kar, N. S., and Bandyopadhyay, S.: Glacial lake outburst flood at Kedarnath, Indian Himalaya: a  
810 study using digital elevation models and satellite images, *Natural Hazards*, 77, 769-786,  
811 10.1007/s11069-015-1629-6, 2015.

812 Dunning, S. A., Rosser, N. J., Petley, D. N., and Massey, C. R.: Formation and failure of the Tsatichhu  
813 landslide dam, Bhutan, *Landslides*, 3, 107-113, 10.1007/s10346-005-0032-x, 2006.

814 Evans, S. G.: The maximum discharge of outburst floods caused by the breaching of man-made and  
815 natural dams, *Canadian Geotechnical Journal*, 23, 385-387, 10.1139/t86-053, 1986.

816 Federal Emergency Management Agency, F.: Direct physical damage—general building stock, HAZUS-  
817 MH Technical manual, chapter5, Federal Emergency Management Agency Washington, DC2004.

818 Furian, W., Maussion, F., and Schneider, C.: Projected 21st-Century Glacial Lake Evolution in High  
819 Mountain Asia, *Frontiers in Earth Science*, 10, 10.3389/feart.2022.821798, 2022.

820 Hugonet, R., McNabb, R., Berthier, E., Menounos, B., Nuth, C., Girod, L., Farinotti, D., Huss, M.,  
821 Dussaillant, I., Brun, F., and Kaab, A.: Accelerated global glacier mass loss in the early twenty-first  
822 century, *Nature*, 592, 726-731, 10.1038/s41586-021-03436-z, 2021.

823 Japan Aerospace Exploration Agency, J.: ALOS World 3D 30 meter DEM (V3.2), OpenTopography  
824 [dataset], <https://doi.org/10.5069/G94M92HB>, 2021.



825 Karra, K., Kontgis, C., Statman-Weil, Z., Mazzariello, J. C., Mathis, M., and Brumby, S. P.: Global land  
826 use/land cover with Sentinel 2 and deep learning, 2021 IEEE international geoscience and remote  
827 sensing symposium IGARSS, 4704-4707,  
828 Komori, J., Koike , T., Yamanokuchi, T., and Tshering, P.: Glacial Lake Outburst Events in the Bhutan  
829 Himalayas, Global Environmental Research ©2012 AIRIES, 16, 12, 2012.  
830 Kropáček, J., Neckel, N., Tyrna, B., Holzer, N., Hovden, A., Gourmelen, N., Schneider, C., Buchroithner,  
831 M., and Hochschild, V.: Repeated glacial lake outburst flood threatening the oldest Buddhist monastery  
832 in north-western Nepal, Natural Hazards and Earth System Sciences, 15, 2425-2437, 10.5194/nhess-  
833 15-2425-2015, 2015.  
834 Liu, K., Song, C., Ke, L., Jiang, L., Pan, Y., and Ma, R.: Global open-access DEM performances in Earth's  
835 most rugged region High Mountain Asia: A multi-level assessment, Geomorphology, 338, 16-26,  
836 10.1016/j.geomorph.2019.04.012, 2019.  
837 Lützow, N., Veh, G., and Korup, O.: A global database of historic glacier lake outburst floods, Earth Syst.  
838 Sci. Data Discuss., 2023, 1-27, 10.5194/essd-2022-449, 2023.  
839 Maurer, J. M., Schaefer, J. M., Russell, J. B., Rupper, S., Wangdi, N., Putnam, A. E., and Young, N.: Seismic  
840 observations, numerical modeling, and geomorphic analysis of a glacier lake outburst flood in the  
841 Himalayas, Science Advances, 6, eaba3645, doi:10.1126/sciadv.aba3645, 2020.  
842 Ministry of Economic Affairs, M.: Bhutan Sustainable Hydropower Development Policy 2021, 2021.  
843 Nagai, H., Fujita, K., Sakai, A., Nuimura, T., and Tadono, T.: Comparison of multiple glacier inventories  
844 with a new inventory derived from high-resolution ALOS imagery in the Bhutan Himalaya, The  
845 Cryosphere, 10, 65-85, 10.5194/tc-10-65-2016, 2016.  
846 National Centre for Hydrology and Meteorology [NCHM].: Reassessment of Potentially Dangerous  
847 Glacial Lakes in Bhutan, National Centre for Hydrology and Meteorology, Royal Government of Bhutan,  
848 Royal Government of Bhutan, PO Box: 2017, Thimphu, Bhutan, 54, 2019.  
849 National Centre for Hydrology and Meteorology [NCHM].: Standard operating procedure (sop) for  
850 GLOF early warning system Punakha-Wangdue valley, National Centre for Hydrology and Meteorology,  
851 Royal Government of Bhutan, Royal Government of Bhutan, PO Box: 2017, Thimphu, Bhutan, 2021.  
852 National Statistics Bureau of Bhutan [NSB].: 2017 Population and housing census of Bhutan, National  
853 Statistics Bureau of Bhutan, Thimphu, Bhutan, 2018.  
854 Nie, Y., Liu, W., Liu, Q., Hu, X., and Westoby, M. J.: Reconstructing the Chongbaxia Tsho glacial lake  
855 outburst flood in the Eastern Himalaya: Evolution, process and impacts, Geomorphology, 370,  
856 10.1016/j.geomorph.2020.107393, 2020.  
857 Nie, Y., Liu, Q., Wang, J., Zhang, Y., Sheng, Y., and Liu, S.: An inventory of historical glacial lake outburst  
858 floods in the Himalayas based on remote sensing observations and geomorphological analysis,  
859 Geomorphology, 308, 91-106, 10.1016/j.geomorph.2018.02.002, 2018.  
860 Nie, Y., Pritchard, H. D., Liu, Q., Hennig, T., Wang, W., Wang, X., Liu, S., Nepal, S., Samyn, D., Hewitt, K.,  
861 and Chen, X.: Glacial change and hydrological implications in the Himalaya and Karakoram, Nature  
862 Reviews Earth & Environment, 2, 91-106, 10.1038/s43017-020-00124-w, 2021.  
863 Nie, Y., Deng, Q., Pritchard, H. D., Carrivick, J. L., Ahmed, F., Huggel, C., Liu, L., Wang, W., Lesi, M., Wang,  
864 J., Zhang, H., Zhang, B., Lü, Q., and Zhang, Y.: Glacial lake outburst floods threaten Asia's infrastructure,  
865 Science Bulletin, 10.1016/j.scib.2023.05.035, 2023.  
866 Petrakov, D. A., Chernomorets, S. S., Viskhadzheva, K. S., Dokukin, M. D., Savernyuk, E. A., Petrov, M.  
867 A., Erokhin, S. A., Tutubalina, O. V., Glazyrin, G. E., Shpuntova, A. M., and Stoffel, M.: Putting the poorly  
868 documented 1998 GLOF disaster in Shakhimardan River valley (Alay Range, Kyrgyzstan/Uzbekistan)  
869 into perspective, Science of The Total Environment, 724, 10.1016/j.scitotenv.2020.138287, 2020.  
870 Petrucci, O.: The Impact of Natural Disasters: Simplified Procedures and Open Problems, in:  
871 Approaches to Managing Disaster, edited by: John, T., IntechOpen, Rijeka, Ch. 6, 10.5772/29147, 2012.  
872 Rahmani, M., Muzwagi, A., and Pumariega, A. J.: Cultural Factors in Disaster Response Among Diverse  
873 Children and Youth Around the World, Current Psychiatry Reports, 24, 481-491, 10.1007/s11920-022-  
874 01356-x, 2022.



875 Rinzin, S., Zhang, G., and Wangchuk, S.: Glacial Lake Area Change and Potential Outburst Flood Hazard  
876 Assessment in the Bhutan Himalaya, *Frontiers in Earth Science*, 9, 10.3389/feart.2021.775195, 2021.

877 Rinzin, S., Dunning, S., Carr, R. J., Sattar, A., and Mergili, M.: Exploring implications of input parameter  
878 uncertainties in glacial lake outburst flood (GLOF) modelling results using the modelling code r.avaflow,  
879 *Natural Hazards and Earth System Sciences*, 25, 1841-1864, 10.5194/nhess-25-1841-2025, 2025.

880 Rinzin, S., Zhang, G., Sattar, A., Wangchuk, S., Allen, S. K., Dunning, S., and Peng, M.: GLOF hazard,  
881 exposure, vulnerability, and risk assessment of potentially dangerous glacial lakes in the Bhutan  
882 Himalaya, *Journal of Hydrology*, 619, 10.1016/j.jhydrol.2023.129311, 2023.

883 Rupper, S., Schaefer, J. M., Burgener, L. K., Koenig, L. S., Tsering, K., and Cook, E. R.: Sensitivity and  
884 response of Bhutanese glaciers to atmospheric warming, *Geophysical Research Letters*, 39, n/a-n/a,  
885 10.1029/2012gl053010, 2012.

886 Sattar, A., Goswami, A., Kulkarni, A. V., Emmer, A., Haritashya, U. K., Allen, S., Frey, H., and Huggel, C.:  
887 Future Glacial Lake Outburst Flood (GLOF) hazard of the South Lhonak Lake, Sikkim Himalaya,  
888 *Geomorphology*, 388, 10.1016/j.geomorph.2021.107783, 2021.

889 Sattar, A., Allen, S., Mergili, M., Haeberli, W., Frey, H., Kulkarni, A. V., Haritashya, U. K., Huggel, C.,  
890 Goswami, A., and Ramsankaran, R.: Modeling Potential Glacial Lake Outburst Flood Process Chains and  
891 Effects From Artificial Lake-Level Lowering at Gepang Gath Lake, Indian Himalaya, *Journal of  
892 Geophysical Research: Earth Surface*, 128, 10.1029/2022jf006826, 2023.

893 Sattar, A., Cook, K. L., Rai, S. K., Berthier, E., Allen, S., Rinzin, S., Van Wyk de Vries, M., Haeberli, W.,  
894 Kushwaha, P., Shugar, D. H., and et al.: The Sikkim flood of October 2023: Drivers, causes and impacts  
895 of a multihazard cascade, *Science*, 0, eads2659, 10.1126/science.ads2659, 2025.

896 Schwanghart, W., Worni, R., Huggel, C., Stoffel, M., and Korup, O.: Uncertainty in the Himalayan  
897 energy–water nexus: estimating regional exposure to glacial lake outburst floods, *Environmental  
898 Research Letters*, 11, 10.1088/1748-9326/11/7/074005, 2016.

899 Shrestha, F., Steiner, J. F., Shrestha, R., Dhungel, Y., Joshi, S. P., Inglis, S., Ashraf, A., Wali, S., Walizada,  
900 K. M., and Zhang, T.: HMAGLOFDB v1.0 – a comprehensive and version controlled database of glacier  
901 lake outburst floods in high mountain Asia, *Earth Syst. Sci. Data Discuss.*, 2023, 1-28, 10.5194/essd-  
902 2022-395, 2023.

903 Taylor, C., Robinson, T. R., Dunning, S., Rachel Carr, J., and Westoby, M.: Glacial lake outburst floods  
904 threaten millions globally, *Nat Commun*, 14, 487, 10.1038/s41467-023-36033-x, 2023a.

905 Taylor, C. J., Robinson, T. R., Dunning, S., and Carr, J. R.: The rise of GLOF danger: trends, drivers and  
906 hotspots between 2000 and 2020, *Authorea Preprints*, 2023b.

907 U.S. Army Corps of Engineers, I. f. W. R., Hydrologic Engineering Center, CEIWR-HEC: HEC-RAS river  
908 analysis system. 2D modeling user's manual, Institute for Water Resources, Hydrologic Engineering  
909 Center, Davis, USA, 289 pp.2021.

910 Uddin, K.: Land cover of HKH region, ICIMOD [dataset], 2021.

911 Uddin, K., Matin, M. A., Khanal, N., Maharjan, S., Bajracharya, B., Tenneson, K., Poortinga, A., Quyen,  
912 N. H., Aryal, R. R., Saah, D., Lee Ellenburg, W., Potapov, P., Flores-Anderson, A., Chishtie, F., Aung, K. S.,  
913 Mayer, T., Pradhan, S., and Markert, A.: Regional Land Cover Monitoring System for Hindu Kush  
914 Himalaya, in: *Earth Observation Science and Applications for Risk Reduction and Enhanced Resilience  
915 in Hindu Kush Himalaya Region: A Decade of Experience from SERVIR*, edited by: Bajracharya, B.,  
916 Thapa, R. B., and Matin, M. A., Springer International Publishing, Cham, 103-125, 10.1007/978-3-030-  
917 73569-2\_6, 2021.

918 Wang, W., Zhang, T., Yao, T., and An, B.: Monitoring and early warning system of Cirenmaco glacial lake  
919 in the central Himalayas, *International Journal of Disaster Risk Reduction*, 73,  
920 10.1016/j.ijdrr.2022.102914, 2022.

921 World Bank, W.: Bhutan - Institutional Strengthening and Modernization of Hydromet and Multi-  
922 hazard Early Warning Services in Bhutan : A Road Map for 2024-2034 (English)Institutional  
923 Strengthening and modernization of hydromet and multi-hazard early warning services in Bhutan: A  
924 road map for 2024 to 2034, 2024.



925 Zhang, G., Bolch, T., Yao, T., Rounce, D. R., Chen, W., Veh, G., King, O., Allen, S. K., Wang, M., and Wang,  
926 W.: Underestimated mass loss from lake-terminating glaciers in the greater Himalaya, *Nature*  
927 *Geoscience*, 10.1038/s41561-023-01150-1, 2023a.  
928 Zhang, G., Carrivick, J. L., Emmer, A., Shugar, D. H., Veh, G., Wang, X., Labedz, C., Mergili, M., Mölg, N.,  
929 Huss, M., Allen, S., Sugiyama, S., and Lützow, N.: Characteristics and changes of glacial lakes and  
930 outburst floods, *Nature Reviews Earth & Environment*, 10.1038/s43017-024-00554-w, 2024.  
931 Zhang, T., Wang, W., An, B., and Wei, L.: Enhanced glacial lake activity threatens numerous  
932 communities and infrastructure in the Third Pole, *Nature Communications*, 14, 10.1038/s41467-023-  
933 44123-z, 2023b.  
934 Zheng, G., Mergili, M., Emmer, A., Allen, S., Bao, A., Guo, H., and Stoffel, M.: The 2020 glacial lake  
935 outburst flood at Jinwuco, Tibet: causes, impacts, and implications for hazard and risk assessment, *The*  
936 *Cryosphere Discuss.*, 2021, 1-28, 10.5194/tc-2020-379, 2021a.  
937 Zheng, G., Allen, S. K., Bao, A., Ballesteros-Cánovas, J. A., Huss, M., Zhang, G., Li, J., Yuan, Y., Jiang, L.,  
938 Yu, T., Chen, W., and Stoffel, M.: Increasing risk of glacial lake outburst floods from future Third Pole  
939 deglaciation, *Nature Climate Change*, 11, 411-417, 10.1038/s41558-021-01028-3, 2021b.  
940 Zhou, H., Wang, J. a., Wan, J., and Jia, H.: Resilience to natural hazards: a geographic perspective,  
941 *Natural Hazards*, 53, 21-41, 10.1007/s11069-009-9407-y, 2009.

942